EFFECT OF THERMAL SHOCK AND LOADING RATE ON THE MICROSTRUCTURE AND PROPERTIES OF Cu/Al_2O_3 COMPOSITES

THIS THESIS IS SUBMITTED IN THE PARTIAL FULLFILLMENT OF THE REQUIREMNT FOR THE DEGREE OF **BACHELOR OF TECHNOLOGY**

IN

METALLURGICAL AND MATERIALS ENGINEERING

BY

SUJASHA GUPTA (Roll No. 109MM0022)

SAVITA GUPTA (Roll No. 109MM0600)

NATIONAL INSTITUTE OF TECHNOLOGY, ROURKELA

NATIONAL INSTITUTE OF TECHNOLOGY ROURKELA

CERTIFICATE

This is to certify that the thesis entitled **"**Effect Of Thermal Shock And Loading Rate On The Microstructure And Properties Of Cu/Al_2O_3 Composites **"** submitted by Sujasha Gupta (109mm0022) and Savita Gupta (109mm0600) in partial fulfilment of the requirements for the award of BACHELOR OF TECHNOLOGY Degree in Metallurgical and Materials Engineering at the National Institute of Technology, Rourkela (Deemed University) is an authentic work carried out by him under my supervision and guidance.

To the best of my knowledge, the matter embodied in the thesis has not been submitted to any other University/ Institute for the award of any degree or diploma.

Date: 9th May, 2012

Prof. Dr. B.C.Ray
Department of Metallurgical and
Materials Engineering,
National Institute of Technology
Rourkela,
Rourkela - 769008

ACKNOWLEDGEMENTS

I avail this opportunity to express my indebtedness to my guide Prof. Bankim Chandra Ray, Head of the Department, Metallurgical and Materials Engineering, National Institute of Technology, Rourkela, for his valuable guidance, allowing access to valuable facilities in the department, constant encouragement and kind help at various stages for the execution of this dissertation work.

I am grateful to Mrs. Khushbu Dash, Department of Metallurgical and Materials Engineering, for providing valuable assistance and insight during the experimental process.

I thank my family and all those friends who helped me in the course of this entire dissertation work.

Sujasha Gupta (109MM0022)

Savita Gupta (109MM0600)

Department of Metallurgical and Materials Engineering,

National Institute Of Technology, Rourkela

Rourkela-769008

ABSTRACT

Metal matrix composites have pervasive applications in automotive and aerospace industries due to excellent properties like high strength to weight ratio which provides excellent weight saving in large components. The copper-alumina composites have high electrical and thermal conductivity coupled with good toughness of copper and hardness of alumina. Nano particulates form stronger and stiffer composites than the micron as they effectively hinder the dislocation movement prohibiting grain coarsening of copper during heat treatment. Thermal shock while in material application plays a dominant role during its performance as it triggers interfacial de-cohesion/cohesion and particle pull out which will check any amelioration or impairment of the properties. 1,3,5 vol.% nano composites and 5,10,20 vol.% micro composites were fabricated by powder metallurgy followed by conventional sintering. Mechanical property determination like micro-hardness measurements, 3-point bend testing was done for thermally shocked specimens under ex-situ and in-situ conditions, followed by characterization under scanning electron microscopy to demarcate the variation in properties. Effect of loading rate on the flexural strengths of the composites was also demonstrated

Keywords: Thermal shock; Interfacial de-cohesion; Microcomposite; Nanocomposite

TABLE OF CONTENTS

LIST OF FIGURES

FIGURE **PAGE**

LIST OF TABLES

TABLE **PAGE**

CHAPTER 1: INTRODUCTION

The metal matrix composites (MMCs) are of keen interest in the recent years because of their extensive application in varied fields of technology [1]. The MMC combines the properties of the metallic matrix and the reinforcement exhibiting enhanced level properties with significant increase of 0.2% yield strength and ultimate tensile strength, toughness, creep strength at higher temperature [1]. The copper alumina composites are extensively used both as functional and structural components. The functional applications mainly comprise of microwaves tubes [2,3], seam welding electrodes and connectors, contact supports, spot welding electrode, oxygen lance nozzle [4-7] and structural applications such as in rocket engine components, automobile and aircrafts parts. In the rocket engine components it is mostly used because of its excellent oxygen compatibility and high thermal conductivity which is essential in the oxygen turbo pumps and ducts thrust chamber lines. However research based on these applications do not take into account the thermal fatigue caused into the components by exposure to varied temperature loading conditions [8]. Thermal shock and thermal cycling of composites play a dominant role during its performance which may either vitiate its performance or ameliorate it [9]. When the MMC is cooled from the fabrication temperature then the matrix shrinks in all directions in relation to the reinforcement, so relative to the "stress-free state" the matrix stretches to maintain the relative continuity with the reinforcement and thus results in "generation of thermally induced micromechanical residual stress" [10].This stress is of primary importance. The matrix and the reinforcement expand and contract at different rates as both have different coefficient of thermal expansion CTE 'α' [9]. So this differential expansion and contraction leads to the generation of thermal stress which affects the microstructural integrity and mechanical properties [11].

Experimentally it is found that a strength weakening in composites is notably conspicuous at high temperature which is directly proportional to $\Delta\alpha$ (α_{matrix}-$\alpha_{reinforcement}$) resulting in diminished fatigues resistance, accelerated stress corrosion, variation in fracture toughness. This can be ascribed to the interfacial de-cohesion and particle pull out arising due to CTE mismatch between them [7].

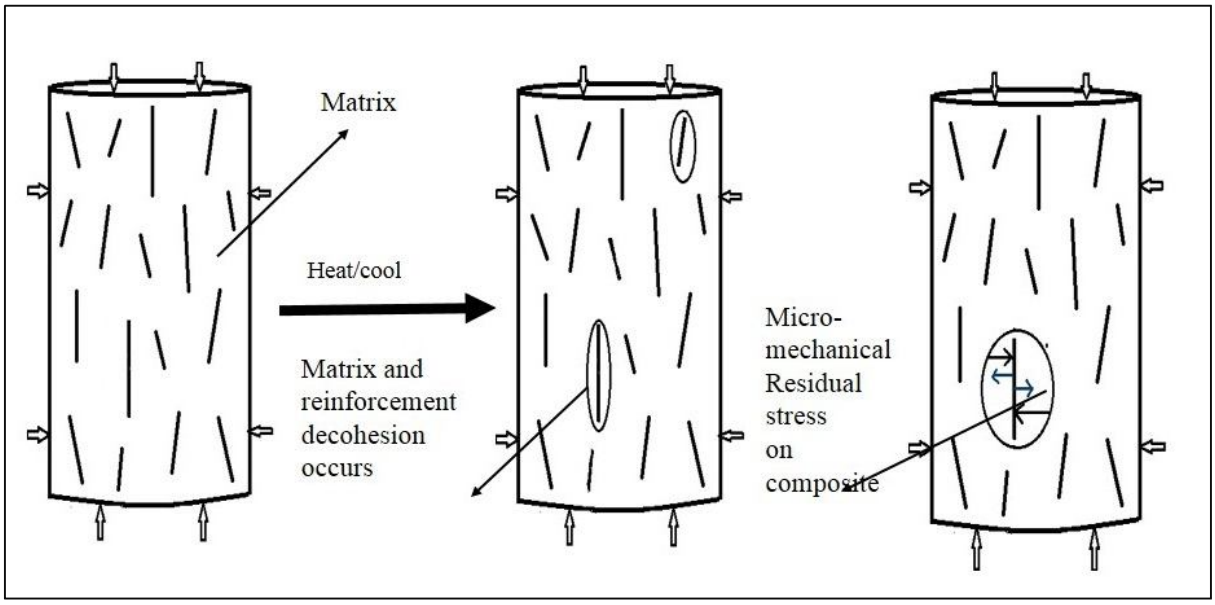

Figure 1 - 4: Illustration of Thermal Shock Phenomena

1.1 Justification of the work:

Copper alumina composites find critical application in Thrust chamber lines of the rocket engines, Propellant management devices (PMD) of the space shuttle main engine and Oxygen lance nozzle. These applications require the composites essentially because of its good oxygen compatibility of the material and high thermal conductivity. Literature study shows that he materials having good oxygen compatibility are copper alloys, iron alloys and nickel alloys. Copper is but preferred because

- Iron alloys have high weight so cannot be used to aerospace and automobiles sector as fuel consumption would be more.

- Nickel can be used but density is 8.5g/cc and compatibility with ceramic composites is poor

- So copper becomes the basis of study.

Literature study shows that for use in oxygen rich environment a material must not support combustion at

- *69 Mpa pressure*

- Have strength of *450 MPa* required at *260^{o}C*

- *Density must be near to 7.5 g/cm3*

In the full flow stages cycle of the Propeller management device shown in fig () below it can be observed here that at one side the ducts and pipes are exposed to fuel which is highly rich environment of oxygen and the other side is exposed to furl rich liquid. So, the part which is exposed to highly rich oxygen fluid needs to be oxygen compatible, i.e. should not ignite in the atmosphere of oxygen, and needs to have strength to support the oxy rich fluid at such high pressures and temperature.

Also, for applications mentioned such as the thrust chamber lines of rocket engine components and the oxygen lance nozzle, it comes in direct contact with a stream of high temperature oxygen. Applications in these require high strength and better creep resistance. Figures are shown below of both the oxygen lance nozzle and thrust chamber lines of rocket engine components.

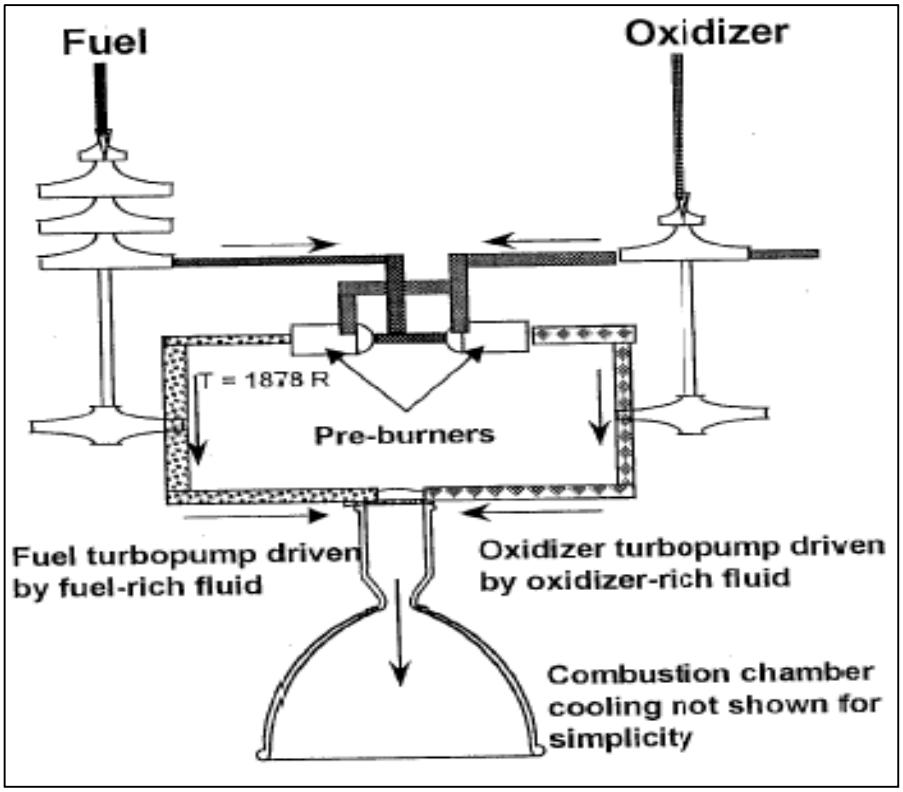

Figure 1 - 2: PMD of the space shuttle main engine showing full flow staged cycle

Figure 1 - 3: Shows the thrust chamber lines of the rocket engine components

Figure 1 - 4: Shows the Oxygen lance nozzle.

CHAPTER 2: LITERATURE REVIEW

2.1 Metal Matrix Composites:

The metal matrix composites (MMCs) are of keen interest in the recent years because of their extensive application in automotive and aerospace industries and other structural applications [1] due to their light weight and better properties with easy availability of reinforcements and predefined fabrication routes giving reproducible properties [2]. Reduction of weight in structural application is not only achieved by reducing the density of the alloy but also by increasing the modulus as done in the Al-SiC composite where a 50% increase in modulus resulted in 10% reduction in weight of the component [3]. Since the MMC combine the metallic properties of ductility and toughness along with the ceramic properties like strength and modulus [4-6] so as stated by Kainer [7] they exhibit enhanced level of properties with significant increase of 0.2% yield strength and ultimate tensile strength, toughness, creep strength at higher temperature, wear resistance, increase in young's modulus than the monolithic component [1]. Since Young's modulus adjustment is necessary as it helps to control noise formation [1]. MMC's can be categorized according to the reinforcement used and in which form they were used as like particulates, platelets, discontinuous/continuous fibres, chopped fibres whiskers, or a network structure in multidirectional direction forming an interpenetrating structure [8-11]. Some early studies on MMC report development of continuous fibre reinforced with mostly aluminium and copper matrices [12-13]. Mattern et al. [14] reports most of the work on MMC's is done on particulate or fibre reinforcements which were not continuous. However, despite such high level properties, problems associated with these mainly are high intensive labour required for the manufacture of these materials, high manufacturing cost associated with some reinforcements giving high end properties,

guaranteeing the interface properties by defining the MMC parameters, optimization of MMC fabrication technology [4,15] so the applications of these materials are limited to only special areas like military and space [4].

2.2 Copper composites:

In the production of copper alumina composites the copper is chosen as the base metal as it has high electrical and thermal conductivity and has comparatively low mechanical properties and is very much used in the engineering areas of electrical and electronics since this element is good conducting powers at elevated temperature. Alumina on the other hand is well known for its exceptionally good high level properties such as good hardness, good inertness to chemical environment, stability in high thermal conditions [16]. The Cu/Al_2O_3 composites especially the alumina dispersion strengthened copper (ADSC) have high electrical conductivity and thermal conductivity in combination with good toughness of copper along with stiffness and hardness of alumina as the matrix retains most of its properties [6,17-18]. The dispersion strengthened MMC has been a subject of interest since 1906 when Wilm discovered age hardening of duralumin [19-20]. Cu/Al_2O_3 dispersion strengthened composites have good mechanical properties both at room temperature and elevated temperature providing creep resistance superior than copper alloys [18, 21]. These are widely used in automobiles and electronics industry. The nano alumina particles are stable upto the melting point of copper and hence inhibit the grain growth but the degradation of the electrical conductivity is minimal due to the low volume fraction of the alumina particles [22-23]. The dispersoids stabilizes the fine substructure formed and inhibits the grain boundary migration [24-29]. Alumina addition has also an added advantage that it can increase the recrystallization temperature as it can pin down the grains and the sub grain boundaries by blocking dislocation movement thereby enhancing the strength at elevated temperatures [16].

2.3 Particulate reinforced composites

In case of particular reinforcements one can get very much attractive properties and hence provide many sustainable material systems since the composites produced can be tailored according to provide isotropic properties in all the three orthogonal directions. Composites with such reinforcements can be produced by customary and also uncustomary methods of fabrication to form a wide range of products and produced in much more cheaper way than with produced with fibres. The properties rendered by particulate reinforcements to the metal matrix depends on the size of the reinforcement, its volume fraction, its distribution, the interparticle spacing, shape and bonding conditions at the matrix and particle interface [30]. Particulate reinforcements chosen can be both of micron size or nano size but most of research done of synthesizing these composites show that nano particulates form more stronger and harder and stiffer composites than the micron particulates as the nano particles are effective enough to hinder the movement of the dislocations within the matrix and also prohibit from grain coarsening of the Cu during its heat treatment [31-33]. These have attracted substantial interest because of the availability of various types of reinforcement at economical expenses and the efficacious progress of manufacturing processes to develop MMCs with reproducible properties and structures [34]. These have shown substantial improvements in terms of strength, stiffness due to their isotropic properties because of which they show excellent performance in extreme loading and thermal conditions (like automotive components).

2.4 Applications of Cu-Al_2O_3 MMC

The copper alumina metal matrix composites are now becoming increasingly important and as good alternatives to be used for functional applications mainly in electrodes for

resistance, microwaves tubes [16], seam welding electrodes and connectors , as conductors for applications involving high temperatures [35-37] , automobile industries [38], as a catalyst in practical lean-burn removal of NO_x as an alternative to the expensive precious metals used.[39], as in electronic packaging , contact supports, in the frictional break parts, electrode materials for the lead wire, spot welding electrode , as the oxygen lance nozzle, other structural applications and thermal management [40] and these applications basically require that the material must possess thermal conductivity high enough and also very low coefficient of thermal expansion which this Cu/Al_2O_3 composite have and these properties can be appropriately controlled by proper metal-ceramic ratio [41].

2.5 Thermal Shock effect

When the matrix is cooled down from the temp of fabrication then the matrix shrinks in all ways which is in relative to the reinforcement. So with relation to its stress –free state the matrix stretches in all directions and maintains its continuity with the reinforcement. Like for instance in case of fiber reinforced material the matrix which is cylindrical in nature stretches axially and also circumferentially [42]. Hence, the matrix goes through a tensile stress state both in the circumferential and axial direction. Therefore this matrix faces a tensile stress state in both axial and circumferential directions. As a result of this expansion and contraction a compressive residual stress acts in the fiber-matrix interface. Whenever composite materials. On the other hand when the composite materials are processed at high and elevated temperatures or when during the times of application they are exposed to high temperature then the differences in the coefficient of thermal expansion and also the elastic constants in the phases would give rise to thermal residual stresses in composites after they are cooled from the exposed high temperature. This gives rise to significant amount of residual stresses in

composites. These influence the material's performance and hence because of that they have stimulated good amount of research and interest [43].

2.6 Micro-mechanical Stresses

On becoming free from external stresses then inside the body in absence of external load stresses act in it. These are called residual stresses or locked-in stresses. These residual stresses can be characterised into three types in accordance to the scale of length over which they act [44]. The type-I stresses are the ones which act over distances which are measured in millimetres and these are referred to as macro-stresses. These develop in material during operations like welding, machining, and other surface finishing operations. The type of residual stresses which are developed in the composites due to the interactions between the reinforcement and the matrix are called type-II stresses. Finally there are stresses which act over atomic scale and vary over the individual grains. These are referred to as type-III stresses. The type-II and type-III are often called collectively are called micro stresses.

These materials are potentially significant for the real-world design and application of these materials [45]. Destructive and non-destructive techniques have been successfully developed to measure residual stresses experimentally. One of the technique has been X-ray diffraction used for calculation of residual stresses in the system of stresses which can exist in a polycrystalline material. The determination of stresses by X-ray diffraction is based on the measurement of lattice spacings of particularly oriented sets of grains using Bragg's law which is given by:

$A = 2dhkl \sin 0$

where A is the wavelength of the incident beam,

dhkl is the interplanar spacing of the crystal plane,

2Θ is the angle between the incident and the reflected beams when a Bragg peak is detected, *hkl* are the Miller indices of the diffracting plane.

These residual stresses have undesirable effects when they are developed. These undesirable effects can include effects like lessened fatigue resistance [46], distortion of shape [47], and accelerated stress corrosion [48]. Moreover the presence, the sign, and the extent of the residual stresses effect considerably the yield strength of the material and also the fracture toughness of the resulting MMCs [49]. For example, prior to the application of external load in the presence of tensile residual stresses in MMCs is often considered as a inherent flaw or defect. Because of the effect of these factors it is not possible to achieve the maximum elastic response of the composites. Presence of tensile the residual stresses may sometimes start and also amplify early damage, such as microcracking, which may happen when the MMCs are mechanically loaded [50]. Formation of residual stresses results into formation of areas of high dislocation density which would be present in a quenched composite and which would suggestively modify the aging nature characteristics of the matrix. It has been studied that the residual stresses which are generated during thermal cycling of MMCs tend to increase the steady state creep rate.

2.7 Powder Metallurgy

In the powder metallurgy technique the particles are mixed together with the reinforcements (here as ceramic particles) and then they are cold compacted in the required forms. For this technique particle size data is essential to treat the powder given. This is helpful for effective distribution of matter and also property developed in the component.

Hence, it can be said particle size distribution is critical for providing the uniformity in the properties. Powder metallurgy is usually followed prior to which blending is done. The

blending is important for the fabrication of MMC. This blending can be termed as a pure and simple operation of mixing two powders, one being atomized alloy powder and other being powder of reinforcement phase. By allowing the effective control in the reinforcement the content of the entire mixture can be controlled. In conventional powder metallurgy based sintering techniques there is no real bonding between the matrix and the reinforcement by any chemical means, due to relatively low temperatures employed for sintering [51]. Good interfacial bonding and proper distribution depend on several parameters like blending speed, blending time, pressure for compaction, particle size variation in the matrix and the reinforcement. Another important factor is the sintering method.

2.8 Sintering

When the thermal energy has been supplied to a powder compact then there occurs densification of compact and the this is followed by increase in the average increase of grain size. Basic phenomena behind sintering can be attributed to

- Densification
- Grain growth

Hence, this can be defined as a processing technique which is used for the production of density controlled materials and components from the powders of metal and ceramic which are when supplied by thermal energy. So, it is considered as one of the basic elements of world of materials science. The various forms of sintering are solid state sintering (where powder is condensed wholly in the solid state), liquid state sintering (liquid phase present in the powder compact during the process of sintering), transient phase sintering and viscous flow sintering. The process of sintering aims to produce reproducible parts and also designs the microstructure

by the control of the many variables, with the main aim being production of fully dense and fine grained structure [52]. The microstructural control occurs by means of

- Control of grain size
- Control of sintered density
- Control the size and distribution of pores.

2.9 Summary

Based on the literature review, the addition alumina powders (nano and micro) have been attempted in copper. Thermal shock effects on these composites have been studied along with the residual stresses generated in the composite. Properties at high temperature have been compared with those of ambient temperature. Further, their additions in different volume fractions and their combination results in varied behaviour under thermal shock effect and this has been explored further by increasing or decreasing their weight content. Also, the fabrication of these composites by conventional sintering technique is considered efficient. Effects of loading rate on the specimens have been studied here. Hardly can it be found in literature about such studies in copper-alumina system. This is completely a newer study and will open an entirely new understanding of the Cu-Al_2O_3 based materials system, believed to be important for various applications. With that as the future idea, the aim of the work undertaken is to investigate the mechanical properties followed by the characterization of the Cu-Al_2O_3 composites.

CHAPTER 3: MATERIALS AND EXPERIMENTAL PROCEDURES

3.1 Overview

In the study, the nano and micro powders of alumina were prepared first by weighing powders of nano-alumina and micro-alumina in their volume fractions by weight along with weighing of copper powder.The copper powder and the alumina powder were then weighed according to the various volume fractions of the reinforcement of 1%,3%,5% for nano-composites composition and 5%,10%,20% for micro-composites. Here the powders after being weighed were blended for 1 hour and then cold compacted with a pressure of 1140 MPa. The compacted pellet of each volume fraction was conventionally sintered for 60 minutes (~900 °C). The sintered pellet was then thermally shocked and high temperature tested at various ranges of temperature. Prior to thermal shock test mechanical and physical property determination was carried out i.e. hardness, density porosity , flexural strength and wear test followed by characterization under scanning electron microscopy (SEM). Ex-situ and in-situ tests were conducted in various ranges of temperature with up treatment from lower to higher temperature and down treatment from higher to lower temperature. The various compositions after being thermally cycled in various temperature ranges underwent mechanical testing methods to demarcate the difference in properties before and after the test. Followed by this the fractured surfaces were observed under scanning electron microscopy to see the matrix particle interface and to check particle matrix debonding has occurred. An approach has been made to calculate the residual stresses developed during the test by the x-ray diffraction microscopy with the help of gravity sliding method and LEPTOS software.

Then, X-ray diffraction was done for the fractured specimens so as to calculate the residual stresses developed in the composite after the ex-situ treatment. Following is the overview of the experimental procedure given.

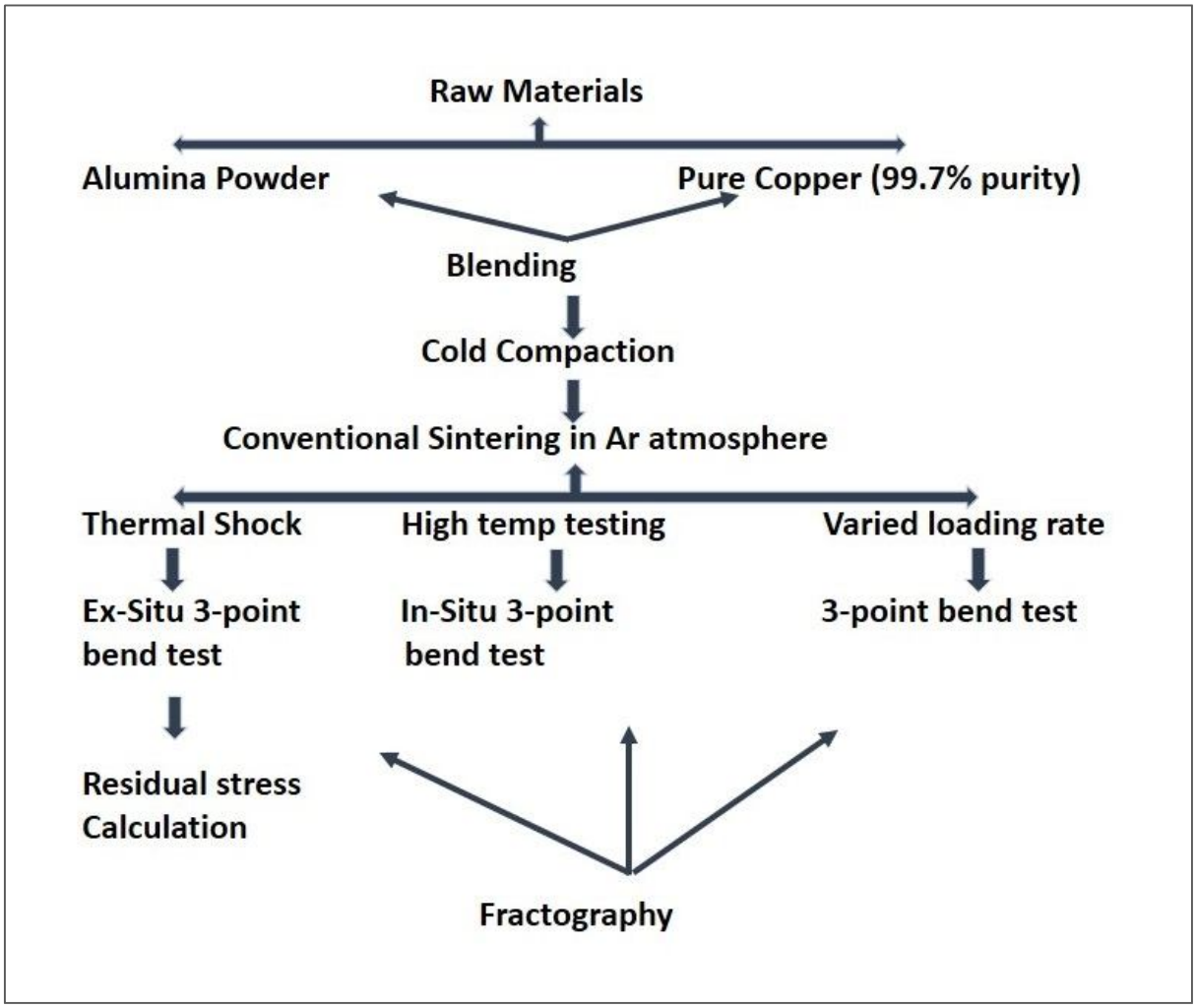

Figure 3 - 5: Overview of Experimental Procedures

3.2 Materials

In this study, the as-received copper (Loba Chemie, purity >99.7%, average size – 11.09 μm) and alumina (Sigma–Aldrich, average size – 5.71 μm and <50 nm) powders were mixed and blended separately using agate mortar for 60 min to ensure homogeneous mixing. Alumina powders of both sizes were mixed with copper powder to prepare the samples. Copper and 1,

3, 5, 7 volume % average size (<50 nm) of nano alumina coupled with 5, 10, 15, 20 volume % of average size (5.71 μm) micron alumina powders were prepared. About 1700 grams of copper, 13.74 grams of nano-alumina powder and 46.34 grams of micro alumina powder were used for the experimental procedure. They were prepared my powder metallurgy (PM) route followed by conventional sintering

Table 3-1 shows the different volume fractions synthesised in this study.

Table 3- 2: Compositions of Materials

Initial Materials	Materials Synthesized
Cu+ 1% Al_2O_3 (nano)	**Cu-1%Al_2O_3**
Cu+ 3% Al_2O_3 (nano)	**Cu- 3%Al_2O_3**
Cu+ 5% Al_2O_3 (nano)	**Cu- 5%Al_2O_3**
Cu+ 5% Al_2O_3 (micro)	**Cu- 5%Al_2O_3**
Cu+ 20% Al_2O_3 (micro)	**Cu -20%Al_2O_3**

3.3 Material Weighing and Calculation of Composition

The weights of the raw materials required were computed prior to processing. The total weight of raw materials for all the samples prepared were 1700 grams of copper, 13.74 grams of nano-alumina powder and 46.34 grams of micro alumina powder. The volume of each sample was maintained constant at 2564.51 mm^3 with a 6.35 mm height, 12.7mm width and 31.8 mm length. The samples prepared were according to the ASTM standard B925-08. The

total powder required for each billet were calculated and then measured using a Setra EL-4100S electronic balance which has an accuracy of 0.01g before packing them separately.

3.4 Primary Processing

First, the weighed powders were cold compacted upto a pressure of 1140 MPa (which is around 19.5 tons). The compacted green pellets were then conventionally sintered in an argon (Ar) atmosphere. The experimental set-up for the compaction and the conventional sintering is shown in Fig 3-2 and Fig 3-3. The experimental procedure is explained in detail below:

Figure 3 - 2: Experimental Set up for Compaction of sample

Figure 3 - 3: Experimental Set up for Sintering

3.4.1 Blending:

Blending is one of the most important parameter to prevent segregation in the Metal Matrix Composites which are produced by powder metallurgy. Before blending the Cu-matrix and Alumina reinforcement powders, the jars were all cleaned. The powders were placed in plastic containers and were neatly sealed. The blending time was kept as 60 mins and the blending speed was maintained at 200rpm.

3.4.2 Cold Compaction:

The prepared powders were then cold compacted. The die and the punch were all cleaned prior to compaction and sprayed with a lubricant zinc sterite. The die and the punch were then set inside the machine in the proper alignment. Compaction was done upto a pressure of 1140 MPa, with a holding time of 120 secs. After this the compacted sample was removed from the die-punch set up by applying pressure, taking care that there is no further application of pressure, thereby removing the sample without no further compaction. The compacted sample was then placed on a crucible inside the sintering set up.

3.4.3 Conventional Sintering:

A sharp furnace was used for sintering the materials. The tubular furnace was kept at 900 ◦C for a holding time of 60 min in argon atmosphere (British oxygen company, 99.994% purity) at a heating rate of 5 ◦C/min The sample was kept inside a pre-calibrated set up, and were heated for 60 minutes at 900 ◦C which is much below the melting point of copper and alumina which are 1083 ◦C and 3000 ◦C respectively . After sintering, the sample is not immediately removed but was allowed to stay for few hours inside the furnace, so as to not to develop any thermal stresses.

3.5 Thermal Shock:

The first set of samples, 1,3,5 volume % of nano-composites and 5,10,20 volume % of micro-composites were then thermally shocked from +80°C to -80°C temperature and from +40°C to -40°C temperature (denoted as down ex-situ test) and the second set of samples were thermally cycled from -80°C to+80°C temperature and from -40°C to +40°C temperature (denoted as up ex-situ test). The following figures will give a clear idea about the treatments done.

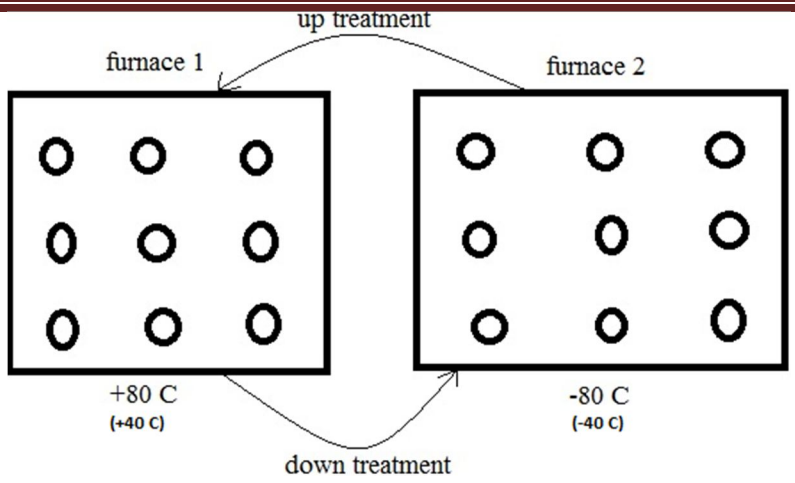

Figure 3 - 4: Shows Ex-situ thermal shock given to the specimens

3.6 Microstructural Analysis

3.6.1. Preparation of samples for microstructural analysis:

Microstructural analyses were carried out on small pellets of 10 mm diameter. The samples were polished with emery paper of 1/0, 2/0,3/0 and 4/0. Once all visible surface scratches and cracks were removed. After paper polishing cloth polishing of samples is done. This is done with the help of brasso liquid. The cloth polishing is then followed by diamond polishing for finer finishing. This is done with the help of diamond spray. The samples would have a mirror-like finish after the polishing process was completed.

3.6.2. Scanning Electron Microscopy (SEM)

Using the SEM JEOL 64480LV Scanning Electron Microscope (SEM), the presence of alumina reinforcement phases was checked and their distribution was also investigated. Images of the microstructure at various magnification and position were captured using an accelerating voltage of 15 kV.

3.7. Mechanical Characterization

3.7.1. Micro-hardness

The micro-hardness values of all the specimens were determined by Vickers hardness tester (Leco LV 700). The readings were recorded here at four equivalent locations for each specimen. The test samples used were cylindrical pellets of 15mm diameter that were flat on both ends and had a mirror-like finish. A diamond vickers indenter was used to make an indentation with an indenting load of 0.3 kgf (2940 mN) and dwell time of 5 seconds. By measuring the size of the indentation, the hardness value was obtained in terms of vickers hardness (HV).

3.7.2 3-point bend test:

Cubical specimens were fabricated by pressing in the compaction machine according to ASTM standard B925-08. The cubicle 3-point bend test specimens have a height if about 6.35mm, width of 12.7mm and a gauge length of 31.8mm. A minimum of 1specimen were fabricated for each composition. The bend test was performed using the INSTRON with a crosshead speed of 0.5 mm/min. A set of flexural stress-strain data was generated during the bend test. The failed tested samples were then unloaded and the fracture surfaces were carefully placed in sealed desiccators, for preventing the surface from contamination. The surfaces were later analysed for their fracture morphology using SEM. The stress-strain data derived from the test was extracted and plotted in Origin.

Figure 3 - 5: Shows the set up for 3-point bend test

Figure 3 -6: Shows the image of sample before and after testing

3.7.2.1. Ex-Situ 3-point Bend Testing:

Cubical test samples were prepared having a height if about 6.35mm, width of 12.7mm and a gauge length of 31.8mm. One set of specimens consisting of 1, 3, 5 volume % of nano-composites and 5, 10, 20 volume % of micro-composites were subjected ex-situ testing. Testing was done at ambient temperature after subjecting the sample to thermal shock. The samples were tested in INSTRON testing machine. The tested samples were then collected. The Engineering Stress-Strain data was then extracted and plotted in Origin Software and comparison of all the compressive data for each composition was done by Origin Software.

3.7.2.2. In-Situ 3-point Bend Testing:

Another set of specimens consisting of 1, 3, 5 volume % of nano-composites and 5, 10, 20 volume % of micro-composites were subjected to In-situ high temperature 3-point bend testing at temperatures around 100^{o}C and 250^{o}C. These samples tested were compared with specimens tested at ambient (25^{o}C) so as to study the difference in flexural strength properties of the composites after the thermal treatment. The experimental set up below shows the set up for the 3-point bend testing and the image of the sample before and after fracture.

3.7.3. Loading rate effect:

The various compositions have been tested here at varied loading rates. Four loading rates have been chosen and the micro and nano composites were tested under such conditions. They were all tested at ambient temperatures. On these compositions the effect of loading rate has been studied with loading rates of 1mm/min, 100mm/min, 500mm/min and 1000mm/min. Variations in flexural properties were seen for all the different compositions.

3.8. Fractography:

Fractography were performed on the fractured surfaces of 3-point bend test tested samples to understand the fracture characteristics of the different compositions under bending stresses. This study was performed using the JEOL 64480LV scanning electron microscope by capturing images at various magnification and positions using an accelerating voltage of 15kV.

CHAPTER 4: RESULTS AND DISCUSSIONS

4.1. Primary Processing

A total of 6 composites of different volume fraction of the reinforcement were produced using the powder metallurgy technique. The nano-composite compositions are Cu-1%Al_2O_3, Cu-3%Al_2O_3, Cu-5%Al_2O_3 and the micro-composite compositions are Cu-5%Al_2O_3, Cu-10%Al_2O_3, and Cu-20% Al_2O_3. The properties of the thermally shocked and high temperature tested specimens were compared the same compositions of composites which are tested at ambient and have no prior thermal treatment done on it. The samples were produced by cold compaction and then were sintered for 60 minutes (900^oC). All samples were successfully compacted and sintered on the first attempt.

4.2. Microstructural Characterisation

The microstructures observed under the scanning electron microscopy (SEM) provides sufficient information regarding the alumina embedment in the copper matrix, the alumina particle and matrix bonding, and the effect of thermal shock on the alumina matrix bonding. The Fig.4-1 - 4-4 shows the embedment of the alumina particles in the copper matrix where the white patches correspond to alumina particles and the grey patches are the copper matrix. We can clearly observe from the SEM micrographs below that the alumina particles have been bonded partially or completely from the copper matrix after the ex-situ thermal shock treatment. However, we can observe from the figures Fig. 4-2 - 4-4 that this bonding is more in case of nano- than micro- composites. This can be attributed to the fact that nano particles have smaller size and effective contact than micron sized particles. So upon thermal shock treatment these nano particles are less pulled out of the matrix than the micron particles giving a better microstructural integrity than the micron particles. Hence, by microstructure-property co-relationship we can say from

the SEM micrographs that nano-composites will be able to retain its property even after harsh changes in its working conditions.

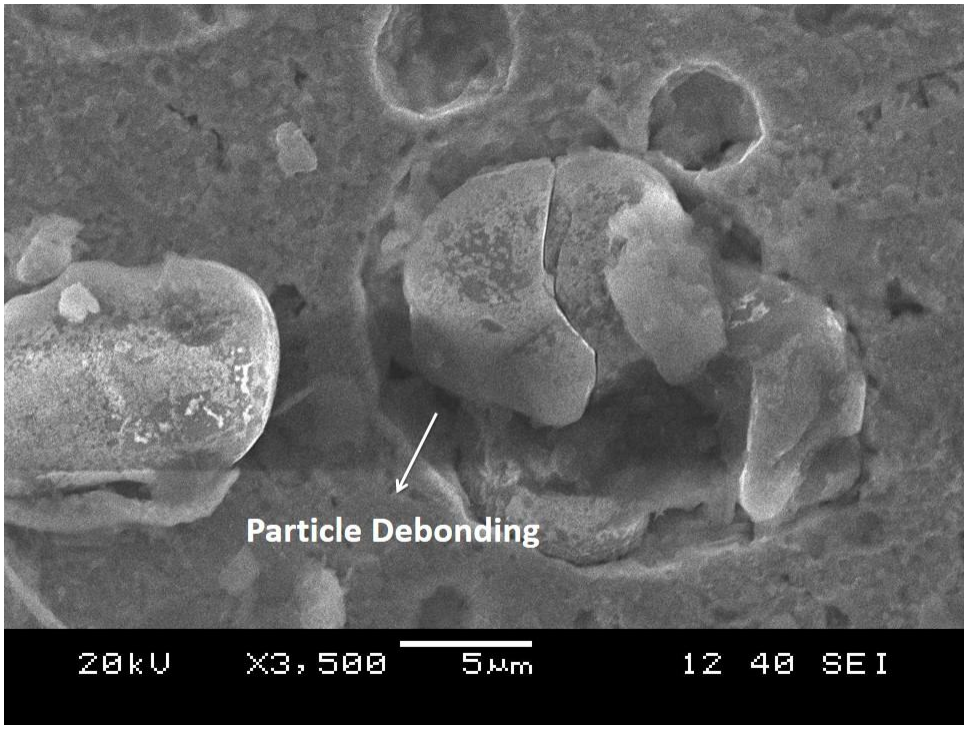

Figure 4 - 6: SEM micrograph of Cu–5 vol.% Al2O3 micro composite sintered under Ar atmosphere, before thermal shock treatment.

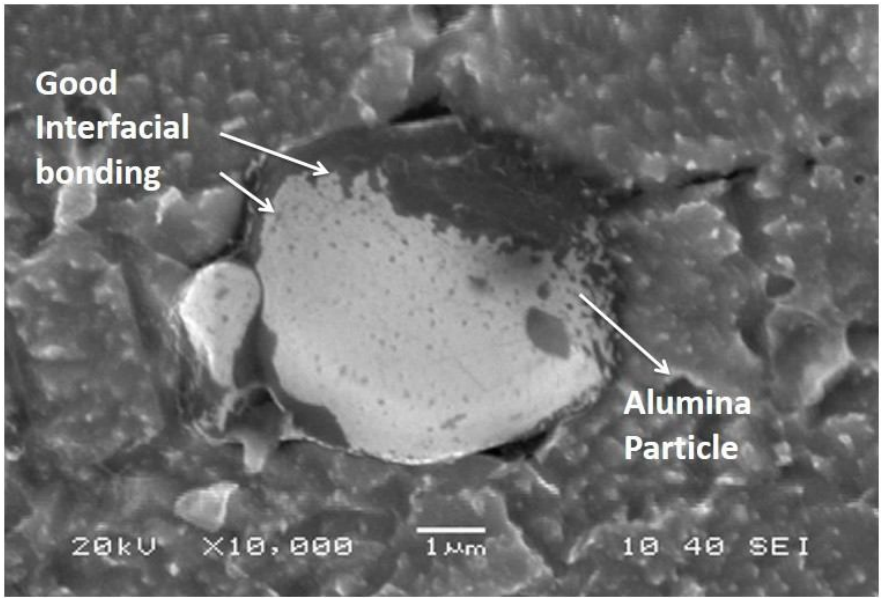

Figure 4 - 2: SEM micrograph of Cu–15 vol.% Al2O3 sintered under Ar atmosphere, after ex-situ up thermal shock treatment.

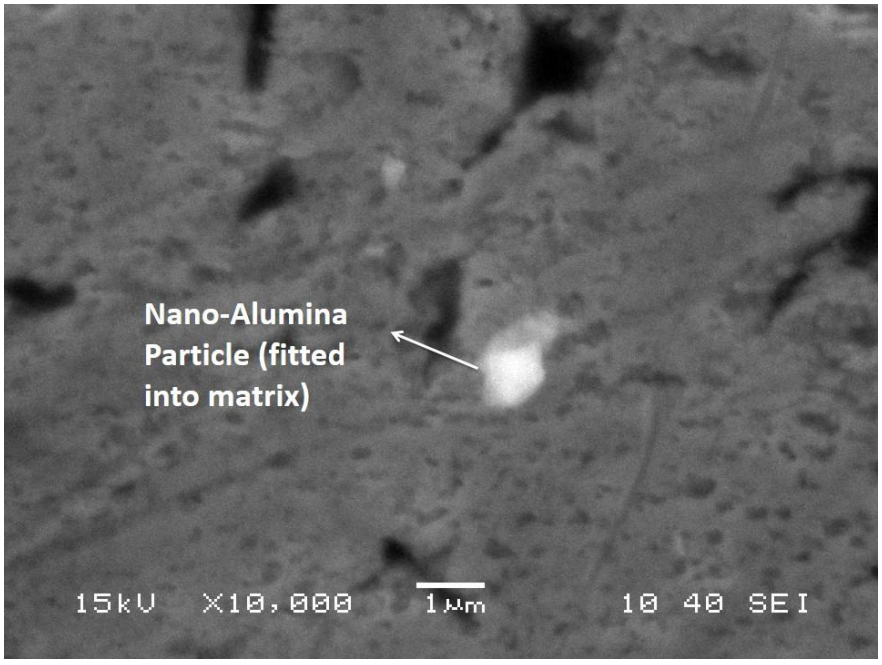

Figure 4 - 3: .SEM micrograph of Cu–5 vol.% Al2O3 nano composite sintered under Ar atmosphere, before thermal shock treatment.

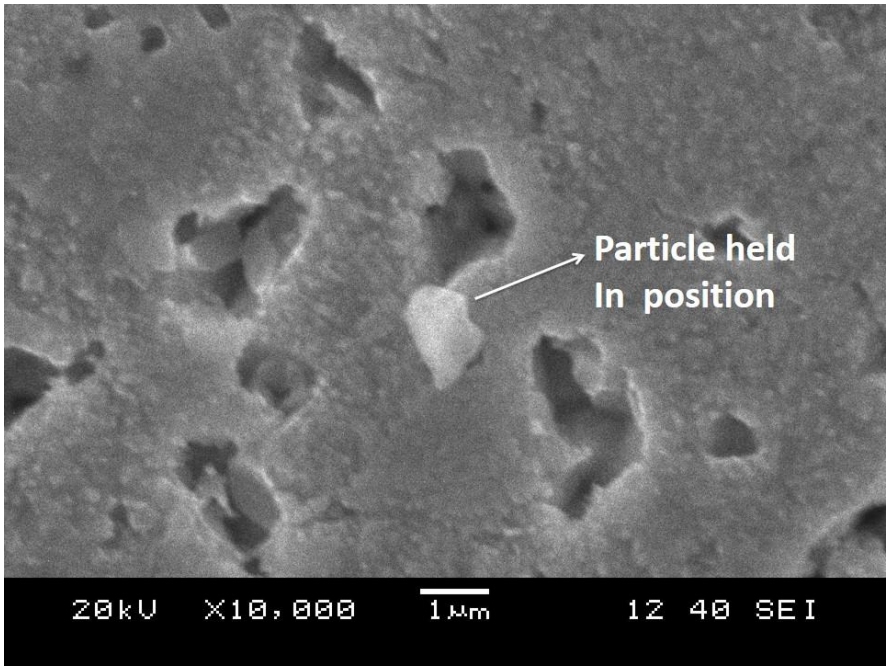

Figure 4 - 4: SEM micrograph of Cu–5 vol.% Al2O3 nano composite sintered under Ar atmosphere, after up ex-situ thermal shock treatment.

4.3. Mechanical Characterisation

4.3.1. Microhardness Test

Results of the microhardness tests are summarised on Table 4-3 for all the compositions of micro and nano composites fabricated.

Table 4- 1: Results of Microhardness Test

MATERIAL	BEFORE THERMAL SHOCK (HV)	AFTER UP THERMAL SHOCK (-80C to +80C) (HV)	AFTER DOWN THERMAL SHOCK (-80C to +80C) (HV)
Cu-1%Al_2O_3 (nano)	53.1± 2.12	72.1±1.9	104.56±6.4
Cu-3%Al_2O_3 (nano)	88.55± 5.04	86.4±5.40	112.62±4.3
Cu-5%Al_2O_3 (nano)	99.8± 5.67	84.5±8.3	98.4±3.2
Cu-5%Al_2O_3 (micro)	84.96±9.31	98.4±3.6	106±8.5
Cu-10%Al_2O_3 (micro)	95.7±11.7	109.6±4.9	117±7.1
Cu-20%Al_2O_3 (micro)	103.4±10.37	90.6± 6.5	95.6±3.8

The datas in the above table are plotted along with the error bar.

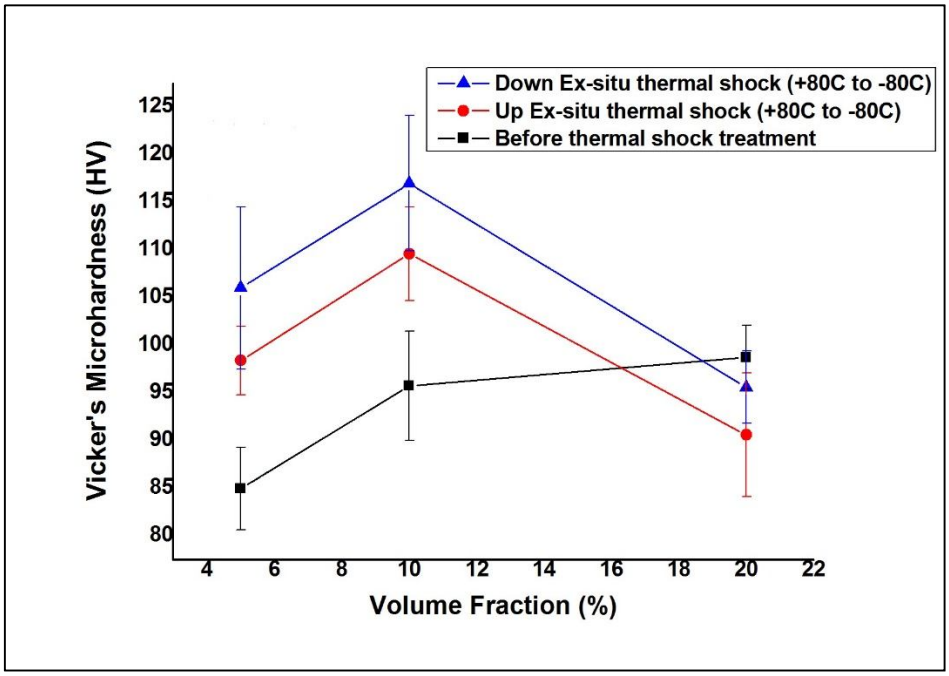

Figure 4-5: Microhardness plots of Cu–Al_2O_3 micro-composite, before and after thermal shock treatment showing both up and down thermal cycle variation.

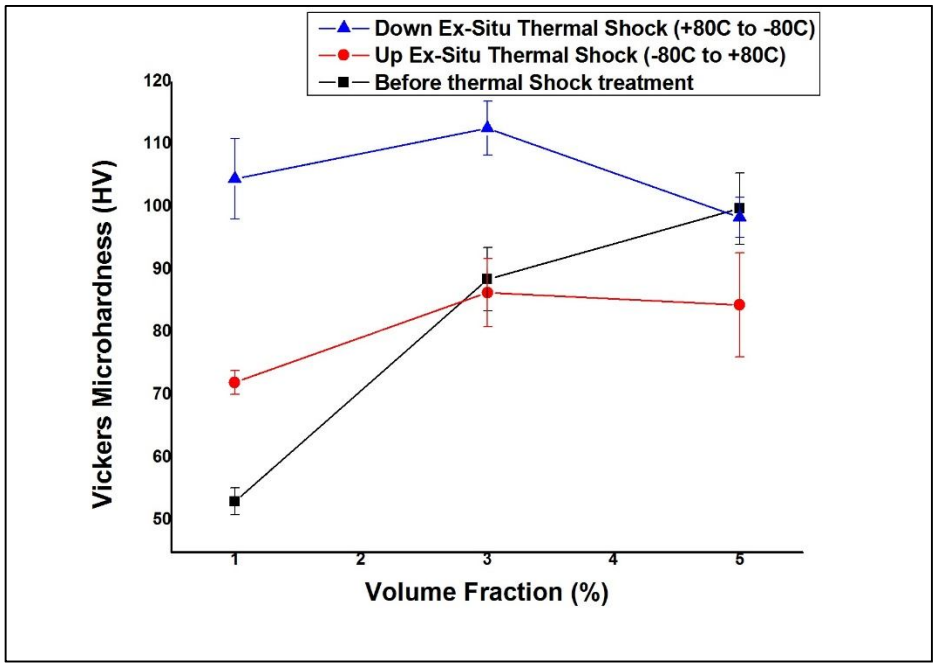

Figure 4-6: Microhardness plots of Cu–Al_2O_3 nano-composite, before and after thermal shock treatment showing both up and down thermal cycle variation.

In both the plots it can be seen that micro-hardness values is increasing for both nano and micro composites after the thermal shock treatment. Due to differential expansion and contraction of the matrix and the reinforcement the bonding between the matrix and reinforcement gets enhanced when there is substantial gap at the particle/matrix interface during the fabrication process. This gap gets bridged due to this phenomena which enhances the microstructural integrity and hence leads to development of the mechanical property and performance

4.3.2. Ex-situ 3-point bend Test:

Following are the results obtained in the Ex-Situ 3-point Bend testing of the samples. All the data of the micro and nano-composites have been tabulated below.

Table 4- 2: Results of Ex-Situ Tests

Volume fraction (%)	Flexural stress at yield (Mpa)	Flexural stress at yield (MPa)		Flexural stress at yield (MPa)	
	Before Shock	***Up(80°C)***	***Down (80°C)***	***Up(40°C)***	***Down (40 °C)***
Cu-1%Al_2O_3 (nano)	222.95	356.93	304.5	430.5	237.77
Cu-3%Al_2O_3 (nano)	238.25	352.76	243.06	328.42	197.94
Cu-5%Al_2O_3 (nano)	175.06	285.71	219.86	296.57	283.31
Cu-5%Al_2O_3 (micro)	143.98	222.87	345.69	165.14	379.44
Cu-10%Al_2O_3 (micro)	186.59	292.45	333.39	231.05	336.4
Cu-20%Al_2O_3 (micro)	108.92	292.14	284.59	183.74	240.56

4.3.2.1. Micro-Composites:

Following are shown the Ex-situ plots of micro composites after the thermal shock treatment. Fig. 4-7(a.b) show the ex-situ plots of micro composites.

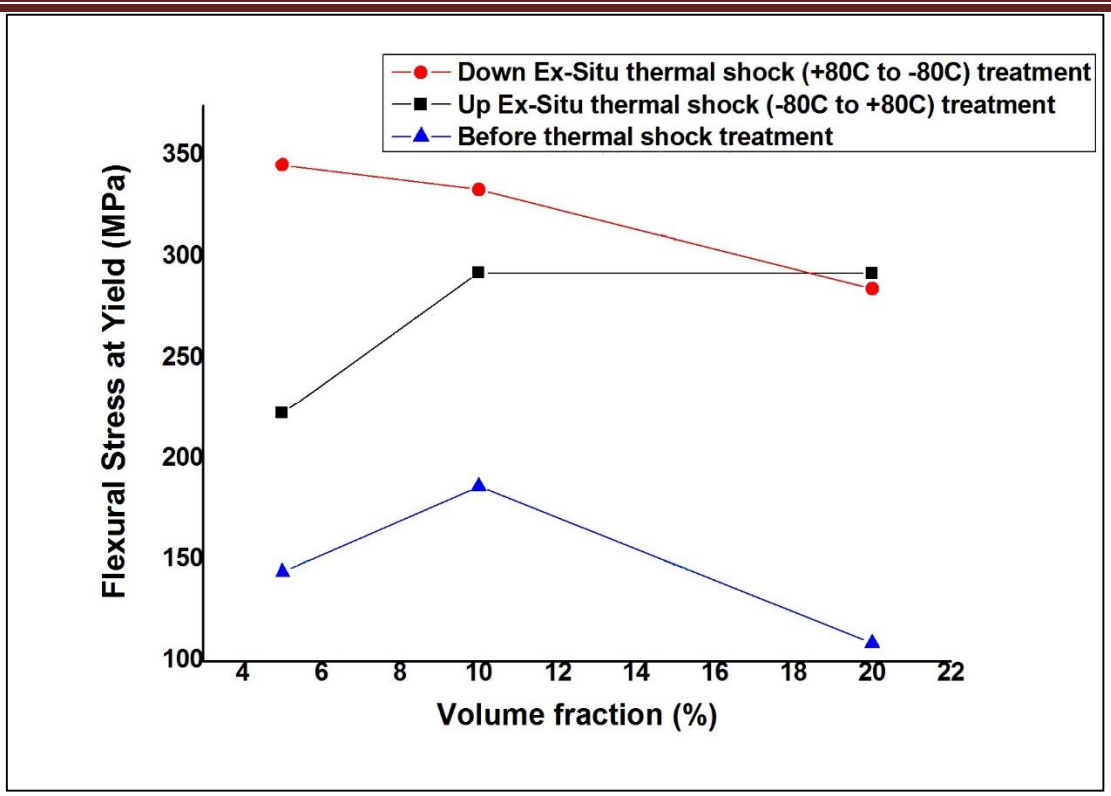

Figure 4 – 7(a): Ex-situ thermal shock testing results for micro composites at ±80°C thermal shock.

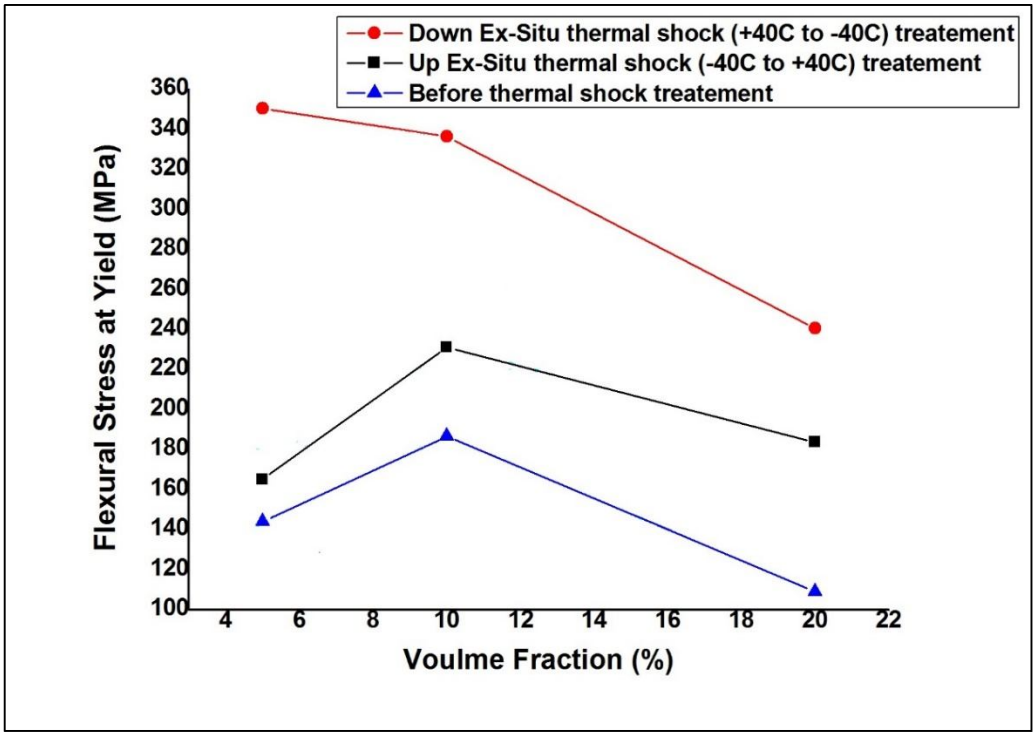

Figure 4 – 7(b): Ex-situ thermal shock testing results for micro composites at ±40°C thermal shock

From fig. 4-7(a) we can't see any variation for up and down thermal at higher volume fraction of Cu-20%Al_2O_3. Properties are better in down ex-situ treatment and decreases as volume fraction increases. During heating matrix expands more than the particle leading to compressive residual stresses but in cooling matrix contracts more than the particle giving rise to tensile shear stresses. Here the matrix gets strain hardened as more dislocations are punched out giving higher mechanical properties during the down treatment. In fig 4-7(b) also we can mark the same trend. Reason is same as in the phenomenon occurring in the down +80°C to -80°C treatment. Flexural strength values are better in this shock test as compared to ± 80°C cycling. This can be attributed to the fact that less degradation of the interface occurs due to the less generation of back stress by the punched put dislocations at the interface. For both the

tests done on the different volume fractions optimum and better values are obtained for Cu-10%Al_2O_3. More the volume fraction of the secondary phase, higher will be the points of defect generations and punching out of dislocations during a thermal shock. With lesser volume fraction of reinforcement the straining of matrix due to generation of defects is less. However, with its increase the matrix gets more strain hardened, leading to increase in mechanical property. But with still higher volume fractions the back stress generated from the defects increases which thereby lowers the properties.

4.3.2.2. Nano-Composites:

Following are shown the Ex-situ plots of nano - composites after the thermal shock treatment.

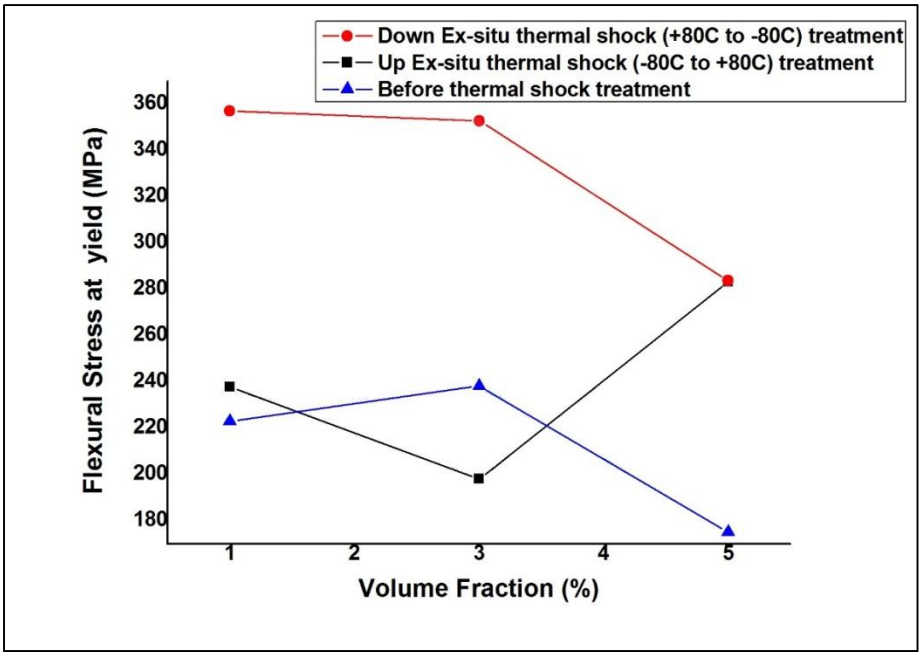

Figure 4 - 8: Ex-situ thermal shock testing results for nano composites at ±80°C thermal shock.

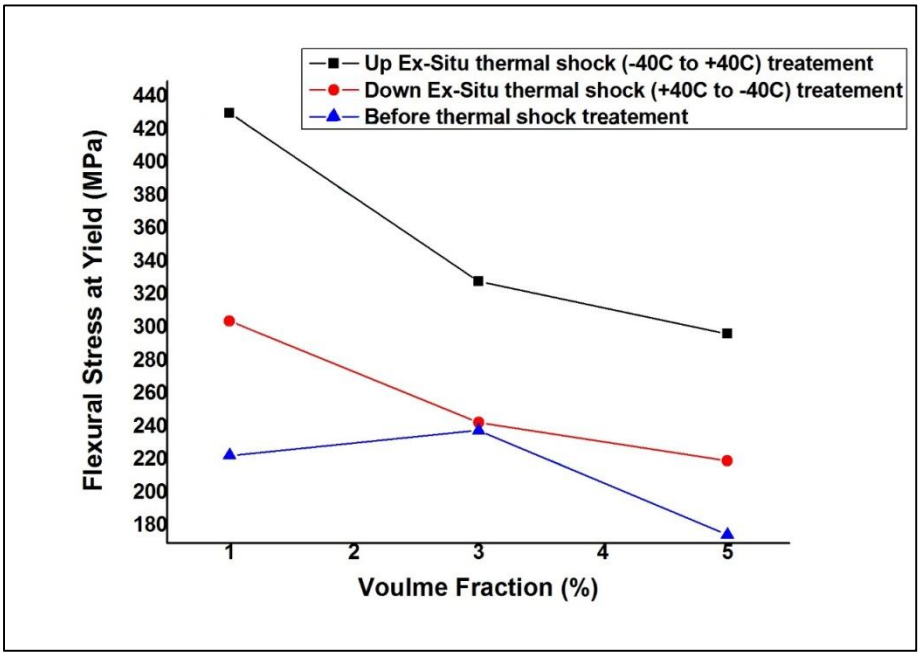

Figure 4 - 9: Ex-situ thermal shock testing results for nano composites at ±40°C thermal shock

From figure 4-8, we can observe maximum variation for volume fraction of Cu-3%Al_2O_3, As reinforcement fractions increases the maximum stresses decrease. This means reinforcement particle doesn't fracture for high volume fractions of reinforcement particle. Change in dominance of damage mechanism from particle fracture at low volume fraction to void formation in highly clustered region. In figure 4-9 maximum variation is seen at volume fraction of Cu-1%Al_2O_3. Nano composites show unlikely different results in this thermal cycle. According to theory and previous results it should show better properties in down thermal treatment. However the trend is just opposite because this temperature range is not sufficient to cause the thermal damage in the composites during the Up ex-situ treatment due to which it gives higher mechanical property as compared to down ex-situ treatment.

4.3.3. In-Situ 3-Point Bend Test

Following are the results obtained in the In-Situ 3-point Bend testing of the samples. All the data of the micro and nano-composites have been tabulated below.

Table 4- 3: Results of In-Situ Tests

Volume fraction (%)	Flexural stress at yield (Mpa)	Flexural stress at yield (MPa)	Flexural stress at yield (MPa)
	At 250 C	***At 100 C***	***At ambient temperature***
Cu-1%Al_2O_3 (nano)	134.96	330.89	222.95
Cu-3%Al_2O_3 (nano)	113.58	360.78	238.25
Cu-5%Al_2O_3 (nano)	268.5	264.58	175.06
Cu-5%Al_2O_3 (micro)	233.26	214.12	143.98
Cu-10%Al_2O_3 (micro)	209.96	191.42	186.59
Cu-20%Al_2O_3 (micro)	203.03	170.36	108.92

Following are the plots shown below for the various compositions In-situ tested.

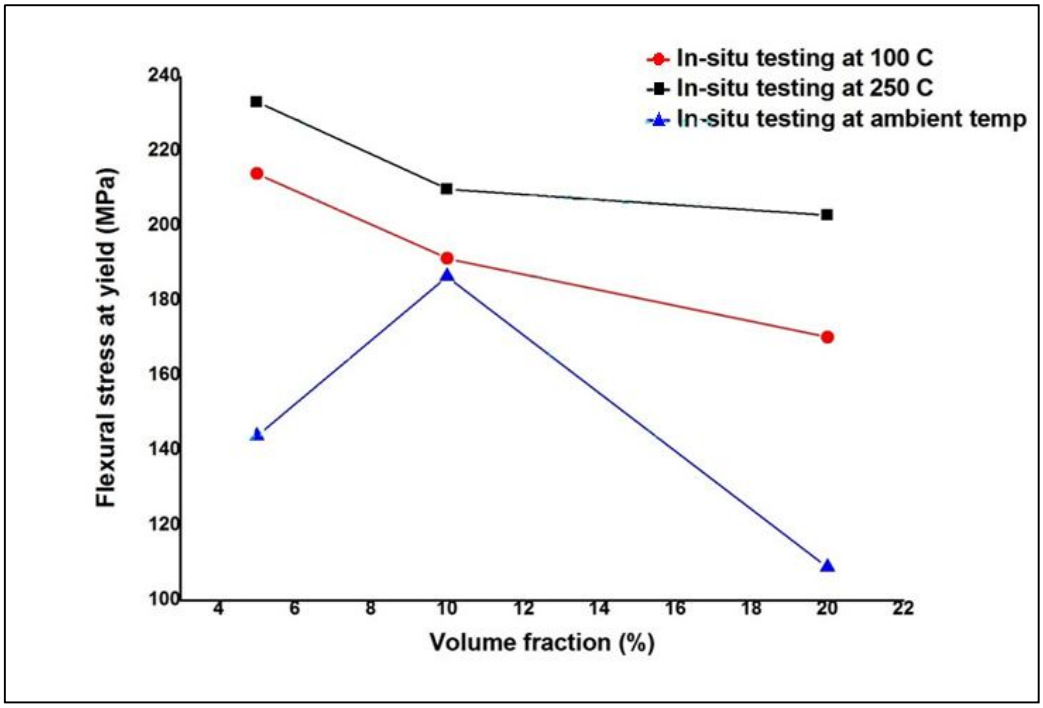

Figure 4-10: In-situ tested flexural properties for micro-composites

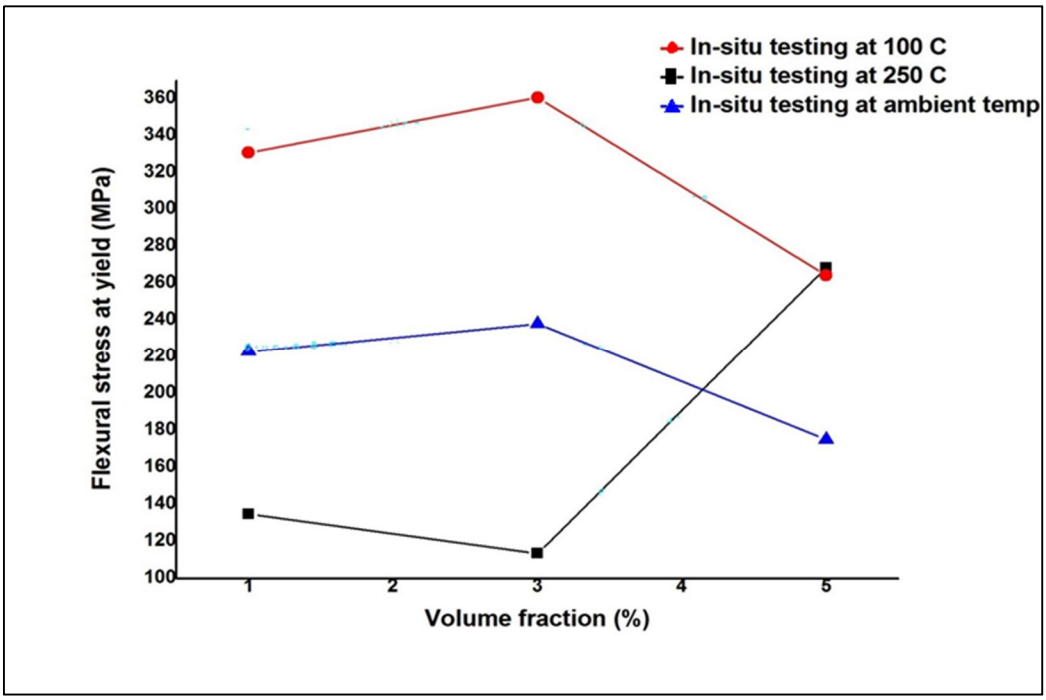

Figure 4-11: In-situ tested flexural properties for nano-composites

Here In-situ testing is done at higher temperatures of 250 ^{o}C and 100 ^{o}C. At higher temp more expansion occurs of the matrix with respect to the reinforcement. There is more thermal stresses generation by this CTE mismatch. These stresses are relieved by plastic deformation of the matrix, leading to strain hardening of the matrix. Variation is observed more for higher volume fraction as when reinforcement fractions increases the maximum stresses decrease. Thus the amount of strain hardening that can occur in matrix due to punching out of dislocations is less leading to lower mechanical properties. Higher values of flexural stress are observed in nano composites at high temp of 100 ^{o}C , as nano particles have more interfacial area with the matrix than the micro particles. Decohesion at the interface due to CTE mismatch occurs by localization of plastic strains at the interface followed by punching out of dislocations. More the dislocation density at the interface more will be the flow stress value. An opposite trend is observed in nano composites as opposed to micro. We get better mechanical properties at 100^{o}C and at 250^{o}C the properties decrease. This can be attributed to the fact that with higher temperature in case if nano-particles substantial debonding occurs at the particle-matrix interface which impairs the microstructural integrity.

However, in case of micro-composites it is observed that the flexural strength gets increases with increase in temperature and decreases with increase in volume fraction. As explained with increase in volume fraction the maximum stresses generated at the interface decreases so properties decreases. But, the flexural strength is higher in higher temperature suggests that at 250^{o}C some bonding is occurring between the matrix and the particle which gives rise to better properties at higher temperatures.

4.3.4. Loading rate rests

Following are the plots of various volume fractions of composites at different loading rates.

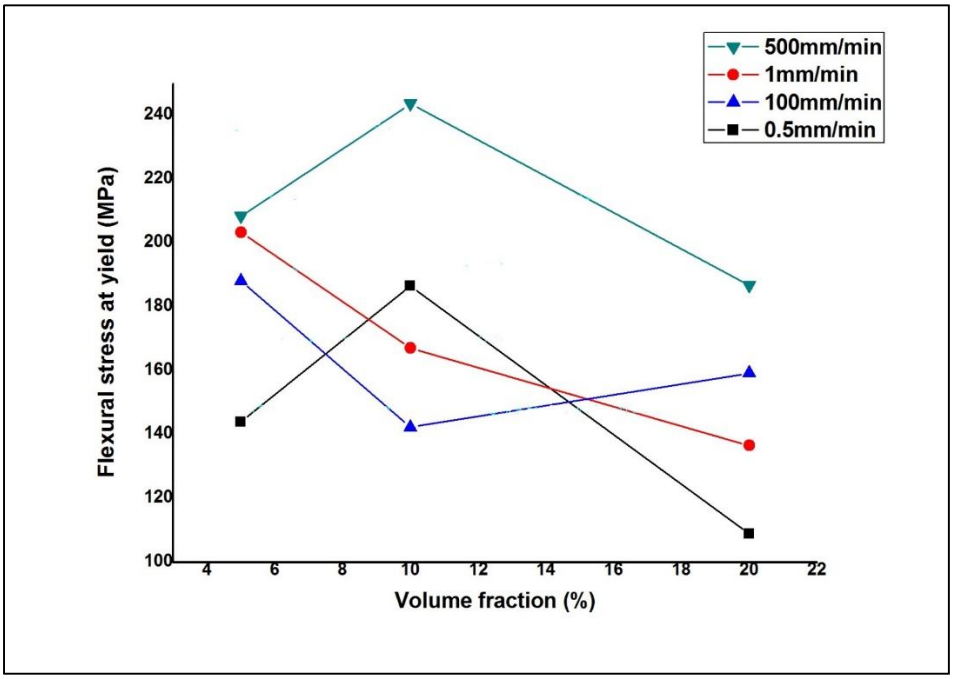

Figure 4-12. Varied loading rate effect on micro-composites

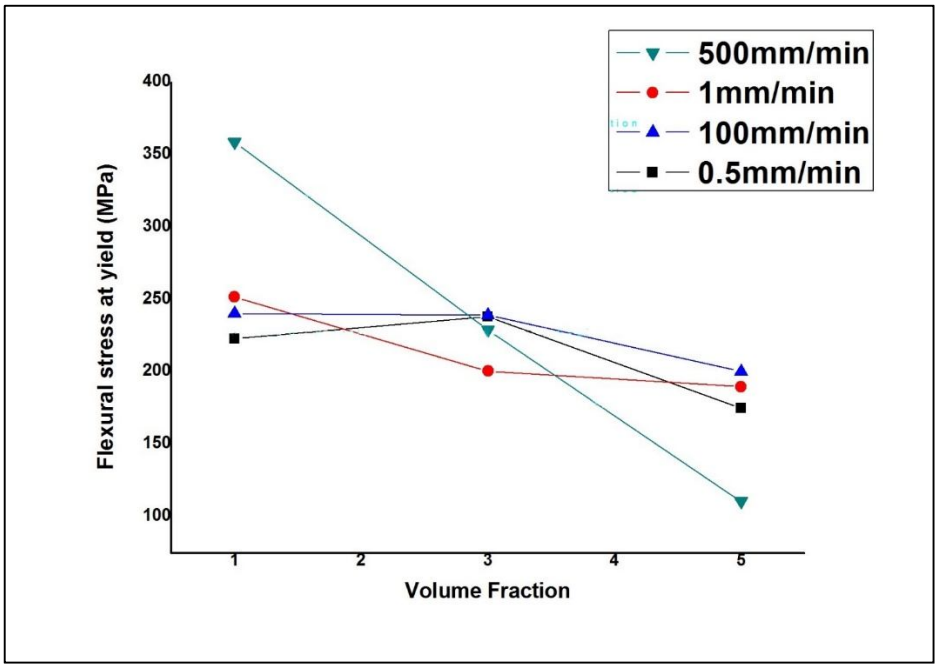

Figure 4-13. Varied loading rate effect on nano-composites

From the stress-strain graphs obtained at varied loading rates it was found that the specimens fractured slowly at higher stresses and low strain rates. This is due to the gradual redistribution of load which becomes possible at slow rate of straining. As a particle fractures the slow rate of straining allows this stress to be transferred to the adjacent particles via the matrix by the distribution of the load. But with the higher strain rate, rapid propagation of the fracture occurs through the matrix, which leads to instantaneous loading of the particles. The failure stress at higher rates of straining or loading decreases as it becomes not possible for the load to be transferred gradually. As found in literature, the final failure of a composite occurs by accumulation of damage. This point gives an explanation of the increase in strength due to increase in loading rate. As, with higher rate of loading, the time of loading decreases, so the time for accumulation of damage decreases, which gives rise to stronger specimens. Here in the figure 4-12 in case of micro-composites highest values of flexural stresses are observed at the loading rate 500mm/min and lowest for 0.5mm/min but these decrease with increase in volume fraction of the composites. Also, for figure 4-13, for Cu-1%Al_2O_3 the maximum stresses occur at 500 mm/min and they drop down in order with decrease in loading rates. However, for higher volume fractions this does not occur. This may be attributed to experimental defects.

4.4. Fractography

Fractography:

The fracture surface morphologies are shown in Figures 4-14 to 4-18. Figure 4-14 shows the fracture surface of Cu-10% Al_2O_3 composite showing dominant ductile fracture, as dimples were observed, in accordance with the failure strain values observed. It is observed in the higher magnification that the bonding between the Cu matrix and the alumina powder is enhanced

after the thermal shock and the particles are intact with the matrix even after failure has occurred due to fracture in the specimen.

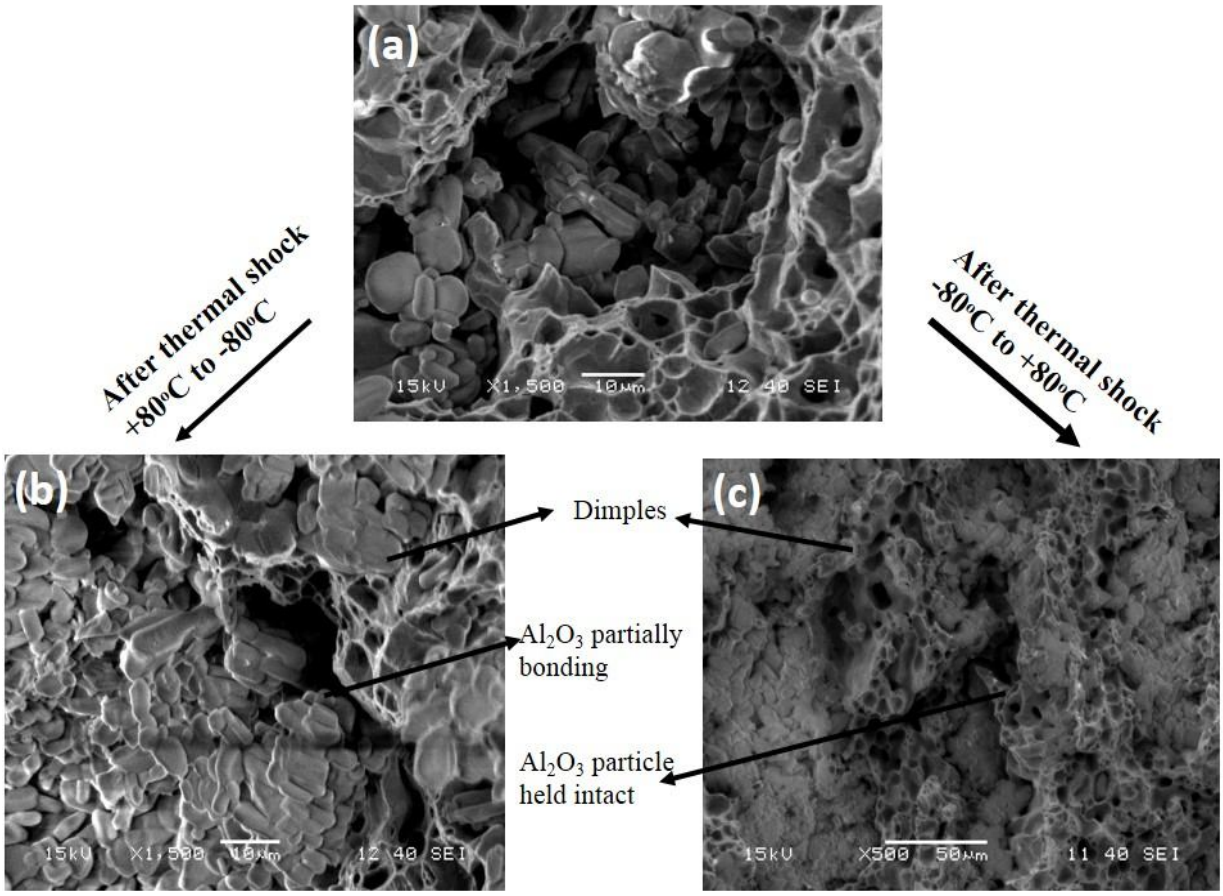

Figure 4-14: Cu-10% Al_2O_3 micro-composite before thermal treatment. (b). Cu-10% Al_2O_3 micro-composite after thermal shock from +80°C to -80°C (c). Cu-10% Al_2O_3 micro-composite after thermal shock from -80°C to +80°C

Bonding and cohesion between the particles is evident from the fractographs after the +80°C to -80°C thermal shock test. The alumina particle embeds itself more into the copper matrix after the shock showing evidence of micro-structural integrity after the shock.

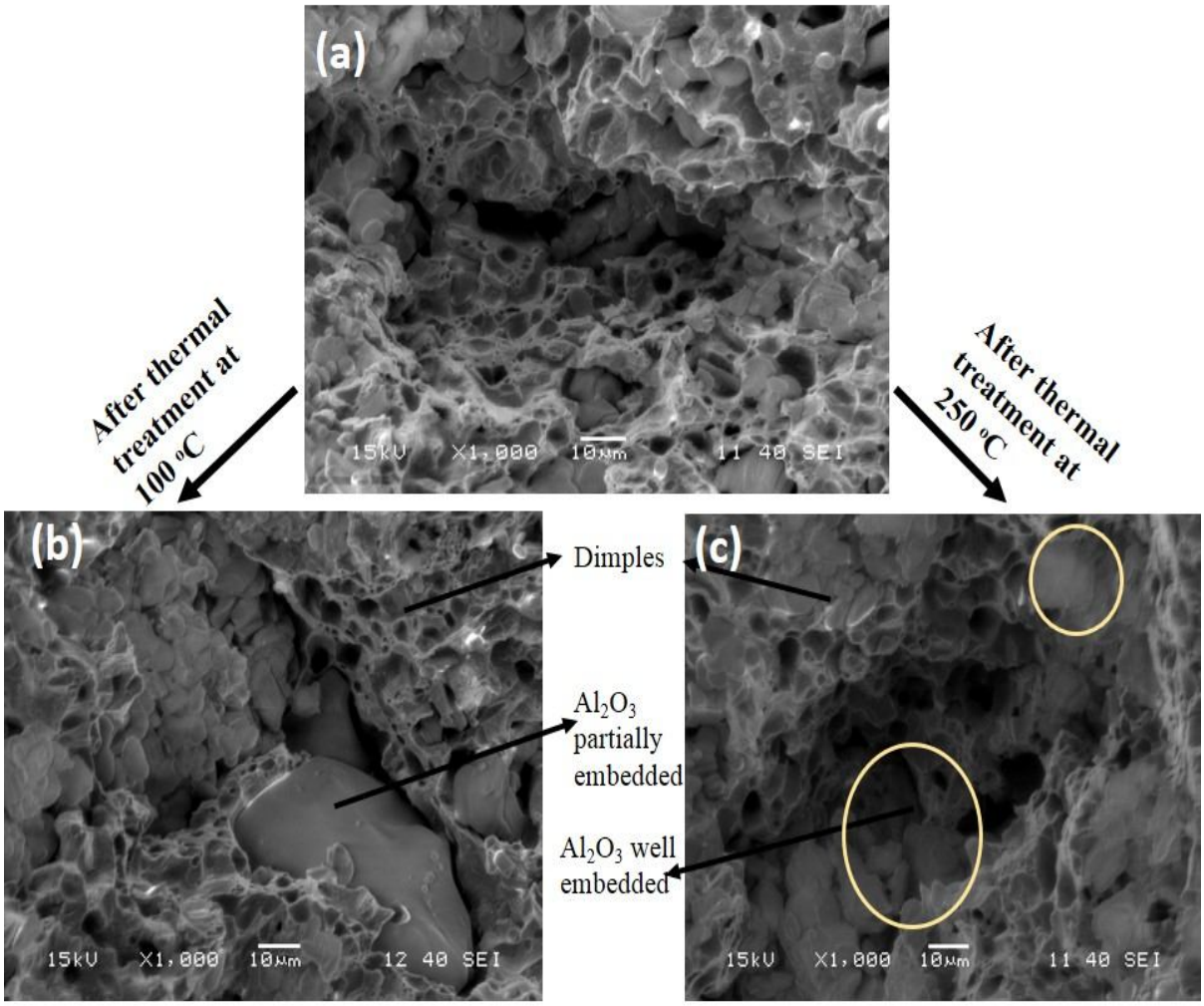

Figure 4-15: Cu-10% Al_2O_3 micro-composite before thermal treatment (b). Cu-10% Al_2O_3 micro-composite after treatment to 100°C. (c) Cu-10% Al_2O_3 micro-composite after treatment to 250°C

In-Situ tested fractograph of the micro-composite Cu-10% Al_2O_3 suggests that alumina particles which were just held in place prior to application of high temperature are now embedding more into the matrix. This was supported by the higher values of flexural strength. With increase in temp increase in embedment of the particles into the matrix is observed.

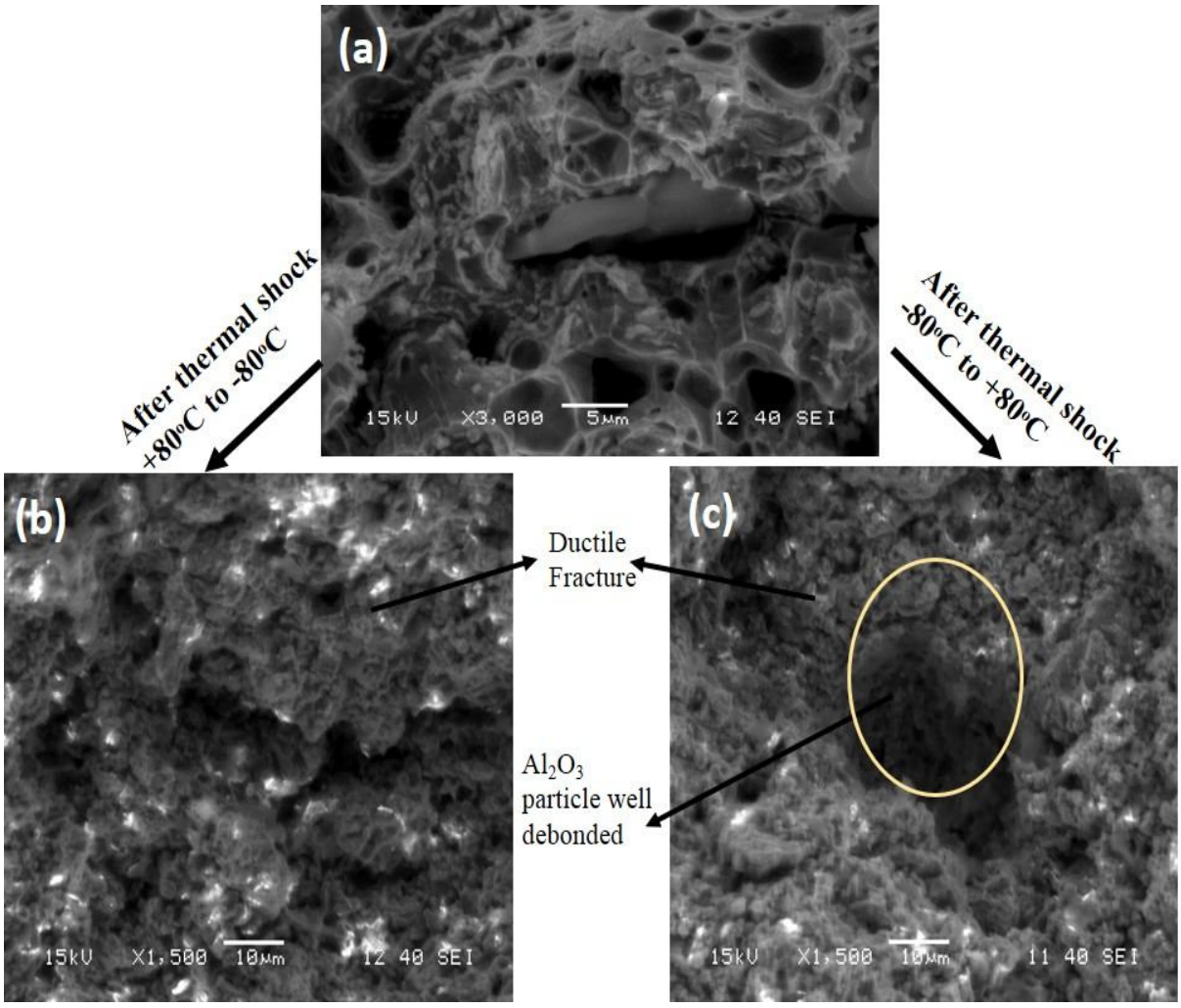

Figure 4-16 Cu-3% Al_2O_3 nano-composite before thermal treatment (b). Cu-3% Al_2O_3 nano-composite after thermal shock from +80°C to -80°C (c) Cu-3% Al_2O_3 nano-composite after after after thermal shock from -80°C to +80°C

Partial debonding has been observed in figure 4-16(a). However, this gap is abridged by the thermal shock phenomena which can be observed in 4-16 (c) where is clearly visible the alumina particle embedding inside the matrix.

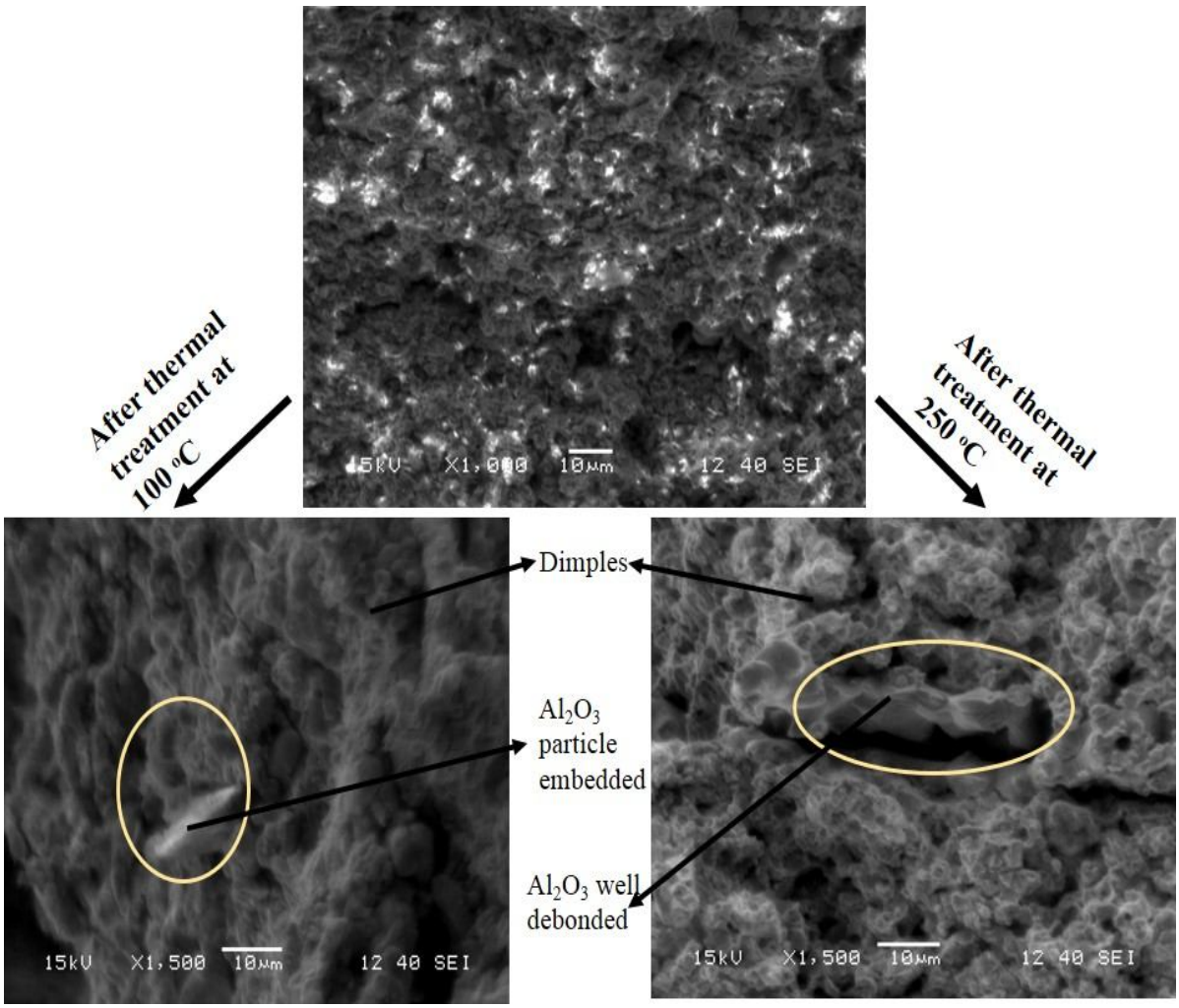

Figure 4-17: Cu-3% Al_2O_3 nano-composite before thermal treatment. (b). Cu-3% Al_2O_3 nano-composite after treatment to 100°C and (c). Cu-3% Al_2O_3 nano-composite after treatment of 250°C.

In this In-Situ tested Cu-3% Al_2O_3 nano-composite we find that alumina particle gets more inside the matrix after the thermal treatment of 100°C. However at 250°C notably decohesion has occurred suggesting interfacial debonding at such a higher temp

4.5. Residual stress Analysis

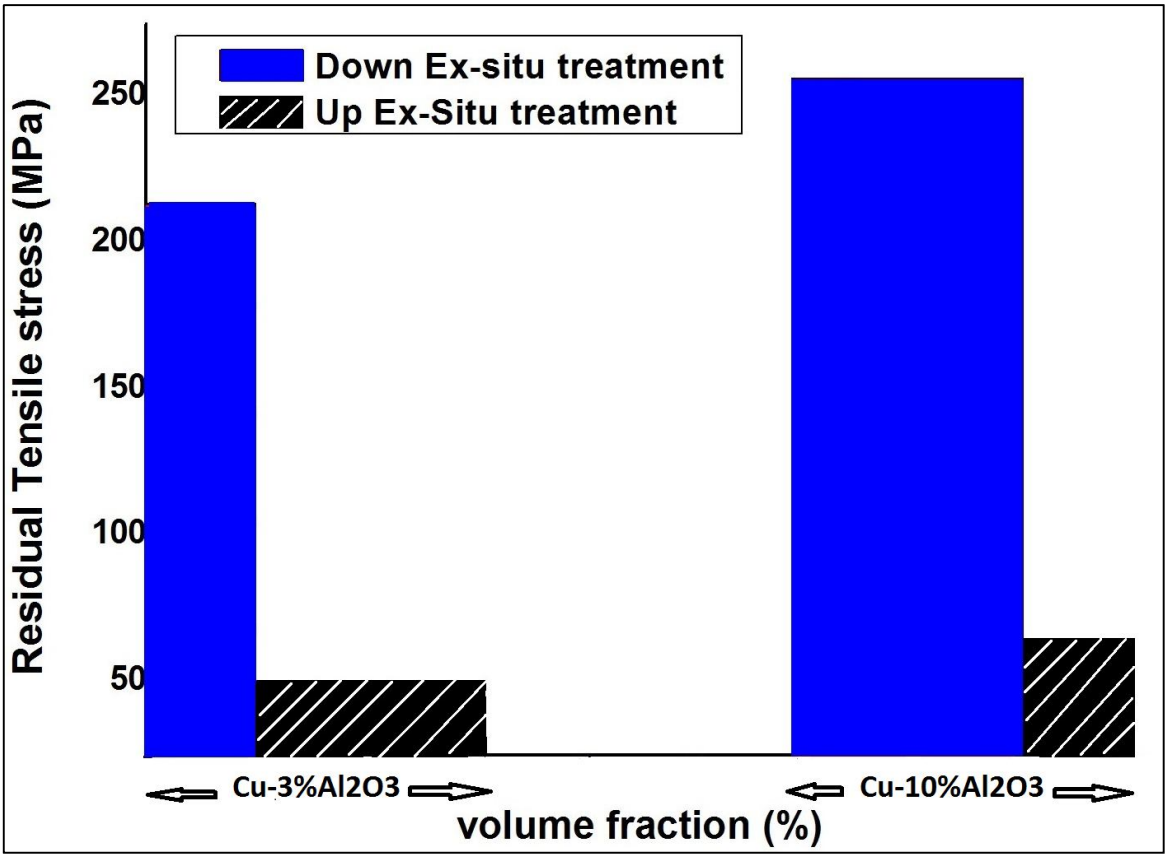

Figure 4-18. Shows residual tensile stress calculation for Cu-10%Al2O3 micro-composite and Cu-3%Al2O3 nano composite

In figure 4-18 We can observe that for down ex-situ thermal shock treatment the residual stress values are more. From the flexural tests it was observed that the max flexural stresses are more for down treatment than up. So, here it can be said that residual stresses help in increasing the properties of the composite.

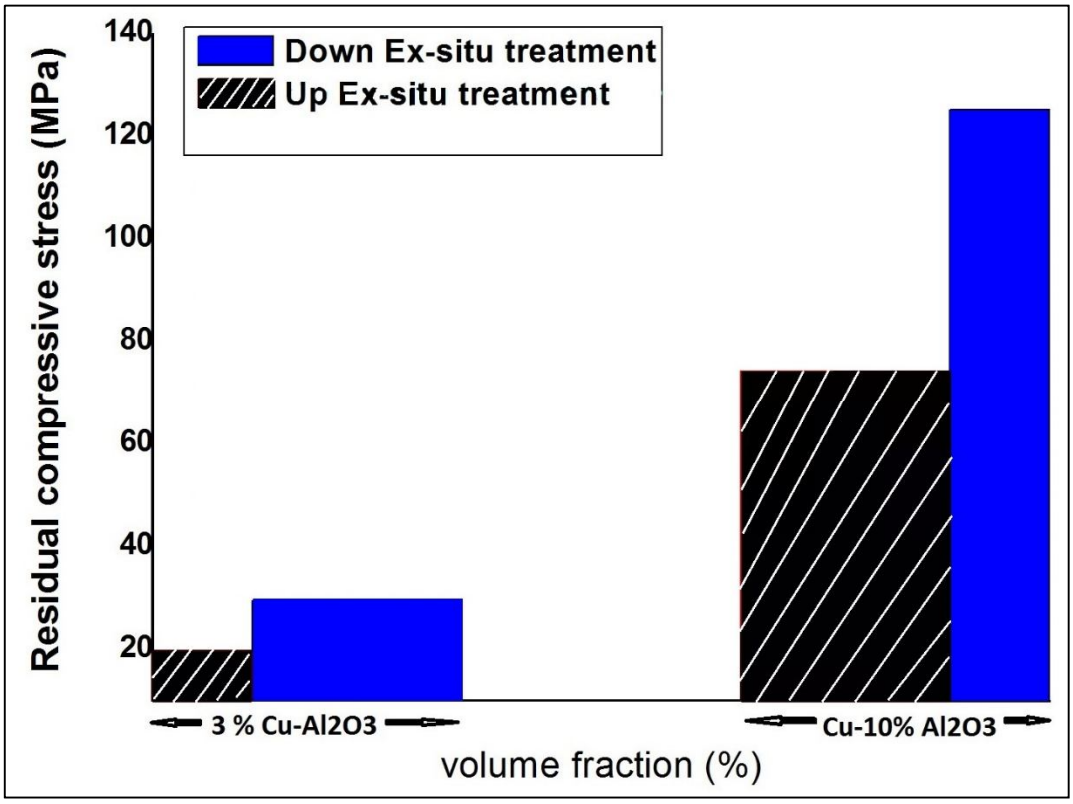

Figure 4-19: Shows compressive residual stress calculation for Cu-10%Al2O3 micro-composite and Cu-3%Al2O3 nano composite

Shows residual stress calculation for Cu-10%Al2O3 micro-composite and Cu-3%Al2O3 nano composite. Both tensile and compressive residual stresses have been calculated by using XRD and LEPTOS software. For Cu-10%Al2O3 residual stress value increases in down ex-situ treatment and has lower residual stresses than the before shock condition. For Cu-3%Al2O3 residual stress value increases too in down ex-situ treatment and has lower residual stresses

than the before shock condition but Up has higher residual stress value than before shock condition.

5. CONCLUSIONS

1. Micro-composites thermal shock and high temperature treatment ameliorates the structure well evident in the fractographs embedding the reinforcements more in the matrix thereby increasing the flexural properties.

2. Residual stress values are also lower in before shock condition.

3. Flexural properties increase with increase in loading rate showing dependence on equations of dislocation density and dislocation velocity

4. Given the higher flexural properties, it provides us a promising solution that the nano-composites can serve as better materials for aerospace and automobile industries where the material is suddenly subjected to high and low temp.

5. Thermal shock and high temp testing study gives us an insight into the changes of the laboratory ambient properties of the materials and better study of phenomena in the materials at such variations of temperature

6. RECOMMENDATIONS

Further works that can be investigated based on the present work are:

1. Repeated tests have to be done to ensure accuracy of the result obtained.

2. Thermal cycling of these metal matrix composites will give better insight about the damage caused due to thermal stresses.

3. Thermal fatigue failure can be conducted to determine the failure mechanism under repeated thermal stresses.

4. Detailed Analysis of the loading rate studies on composites.

REFERENCES

1. [F. Scherma, R. Volkla, S. van Smaalena, S. Mondala, P. Plamondonb, G. Li Esperance, F. Bechmann, U. Glatzel , Microstructural characterization of interpenetrating light weight metal matrix composites, Materials Science and Engineering A 518 (2009) 118–123
2. T.W. Chou, A. Kelly and A. Okura, Composites 16 (1986) 187.
3. A.P. Divecha and S. G. Fishman, ,Mechanical Properties of Silicon Carbide Reinforced Aluminum, in Proc. 3rd Int. Conf. on Composite Materials, Vol. 3, 1979, 351.
4. A.Ibrahim, F.A.Mohamed, E.J.Laverni, Particulate reinforced metal matrix composites- a review, Journal of Materials Science 26(1991) 1137-1156
5. M. Knechtel, H. Prielipp, H. Mullejans, N. Claussen, J. Rodel, Mechanical properties of Al/Al2O3 and Cu/Al2O3 composites with interpenetrating networks, Scripta Metallurgica et Materialia 31 (1994) 1085–1090.
6. Jami Winzer, Ludwig Weiler, Jeanne Pouquet, Jurgen Rodel, Wear behaviour of interpenetrating alumina–copper composites Wear 271 (2011) 2845– 2851.
7. K.U.Kainer, in: K.U.Kainer (Ed.), Metal Matrix Composites, Wiley-VCH, Weinheim, 2006,pp.1-52.
8. H.Y.Wang, Q.C. Jiang, Y.Q. Zhao, Mater. Sci. Eng. A 372 (2004) 109.
9. Z.Trojanova, P.lukac, W.Riehemann, B.L.Mordike, Mater.Sci.Eng A324 (2002) 122.
10. Z.R.Xu, K.K.Chawla, A.Wolfenden, A.Neuman, G,M,Ligget, N.Chawla, Mater. Sci.Eng. A 203 (1995) 75
11. A.L.Geiger and M.Jackson, Adv. Mater. Process 7 (1989) 23

12. A.K. DHINGRA, J. Met. 38 (1986) 17.
13. R.C. FORNEY, ibid. 38 (1986) 18.
14. A. Mattern, B. Huchler, D. Staudenecker, R. Oberacker, A. Nagel, M.J. Hoffmann, J. Eur. Ceram. Soc. 24 (2004) 3399.
15. A. A. Zabolotsky, Structure and properties formation of metal matrix composites, Composites Science and Technology 45 (1992) 233-240.
16. Sintered Materials Based on Copper and Alumina Powders Synthesized by a Novel Method, M. Korac, Z. Kamberovic, Z. Andjic, M. Filipovic, M. Tasic, Science of Sintering, 42 (2010) 81-90
17. Amir Afshar, A. Simchi, Flow stress dependence on the grain size in alumina dispersion-strengthened copper with a bimodal grain size distribution, Materials Science and Engineering A 518 (2009) 41–46
18. Govind, R. Balasubramaniam and G.S. Upadhyaya, Elevated temperature deformation behaviour of alumina-dispersed P/M copper, Materials Chemistry and Physics, 36 (1994) 371-376
19. A. Wilm, Metallurgie. 1911. 8. 225.
20. Majumder, Thin Solid Films. 1995. 42. 327-341p.
21. Sintering of copper-alumina composites through emending and mechanical annoying powder metallurgy routes, Anish Upadhyaya, G. S. Upadhyaya, Materials & Design Volume 16 Number 1 1995.
22. A.V.Nadkarni, J.D. Troxell, F. Verniers, GlidCop Dispersion Strengthened Copper:An Advanced Alloy System for Automotive and Aerospace Applications, Report SCM Metal Products Inc., Cleveland, Ohio, 1989.
23. S.-H. Kim, D.N. Lee, Mater. Sci. Eng. A 15 (1999) 352–354

24. F.J. Humphreys and J.W. Martin, Phil. Mug., 17 (1968) 365.
25. I. Baker and J.W. Martin, in N. Hansen, A.R. Jones and T. Leffers (eds.), Proc. 1st Rird Int. Symp. Metallurgy and Materials Science, Risd National Laboratory, Roskilde, 1980, p. 27.
26. J. Naser, H. Ferkel, W. Riehemann, Mater. Sci. Eng. A, 234-236 (1997) 470.
27. Z. Trojanová, H. Ferkel, P. Luká, J. Naser, W. Riehemann, Scr. Mater., 40 (1999) 1063.
28. M. Korac, Z. Kamberovic, Z. Andjic, M. Filipovic, M. Tasic, Sintered Materials Based on Copper and Alumina Powders Synthesized by a Novel Method, Science of Sintering, 42 (2010) 81-90
29. B. Tian, P. Liua, K. Songa, Y. Lia, Y. Liua, F. Rena, J. Sua, Mater. Sci. Eng. A, 435-436 (2006) 705.
30. Processing of discontinuously reinforced Metal matrix composites by rapid solidification, T.S. Srivatsan, T.S.Sudarshan, E.J.Lavernia, , Progress-in-Materials-Science, Vol 39, 1995 , 317-409
31. Manufacturing nano-alumina particle-reinforced copper alloy by explosive Compaction Zhao Zheng, Li Xiao-jie, Tao Gan. Journal of Alloys and Compounds 478, 2009, 237-239.
32. Properties of copper matrix reinforced with nano and micro sized alumina particles, Visessleva Rajkovic, Dusan Bozic, and Milan T.Jovanovic. Journal of Alloys and Compounds 459 (2008) 177–184.
33. Synthesis and characterization of copper alumina metal matrix composite by conventional and spark plasma sintering, K.Dash, B.C.Ray, D.Chaira. Journal of Alloys and Compounds 516 (2012) 78– 84.

34. In-Jin Shon, et al. Electronic Materials Letters. 2009. 5 (2). 77-81p

35. A.V.Nadkarni, in: E. Ling (Ed.), High Conductivity Copper and Aluminum Alloys, Metall. Soc. AIME,Warrendale, PA, 1984, pp. 77–101

36. P. Sudharshan Phani, V. Vishnukanthan, G. Sundararajan, Effect of heat treatment on properties of cold sprayed nanocrystalline copper alumina coatings, Acta Materialia 55 (2007) 4741–4751

37. M.X. Guo, et al. Material Characterization. 2007. 58. 928-935p.

38. Xiao Yong, et al. Procedia Engineering. 2012. 27. 880 – 886p

39. Masakuni Ozawa, et al. Applied Surface Science . 1997. 121 / 122 441-444p.

40. Y. Tamaka and M .Noguchi. Weld Int .1987. 1(11). 1074p

41. C.A. Leon, et al. Materials Science and Engineering A. 2009. 526. 106–112p.

42. S. Ho and E. J. Lavernia, "Thermal Residual Stresses in Metal Matrix Composites: A Review", Applied Composite Materials ,2, (1995), 1-30.

43. Kalpakjian, S., "Manufacturing Processes for Engineering Materials", Addison-Wesley Publishing Company, Reading, MA, (1985)

44. Eigenmann, B., Scholtes, B., and Macherauch, E., Mater ScL Eng. All8, 1989, 1.

45. Povirk, G. L., Stout, M. G., Bourke, M., Goldston, J. A., Lawson, A. C., Lovato, M., Macewen, S. R., Nutt, S. R., and Needleman, A., Acta Metall. Mater. 40, 1992, 2391.

46. Wiesner, C., Metall. Trans. 23A, 1992, 989.

47. Tszeng, T. C., PhD Dissertation, University of California, Berkeley, 1987.

48. Kalpakjian, S., Manufacturing Processes for Engineering Materials, Addison-Wesley Publishing Company, Reading, MA, 1985.

49. Clegg, W. J., Acta Metatl. Mater. 36, 1988, 2141.

50. Penn, L. S., Chou, R. C. T., Wang, A. S. D., and Binienda, W. K., J. Compos. Mater 23, 1989, 570.
51. Hot pressing of aluminium or aluminium-copper-alumina short fibre reinforced composites, M.EMormo et al. Banloche Atmmc Centre, Argentina. PowderMetall., Vo143, No 1, 2000. 83-88.
52. Processing of discontinuously reinforced Metal matrix composites by rapid solidification, T.S. Srivatsan, T.S.Sudarshan, E.J.Lavernia, , Progress-in-Materials-Science, Vol 39, 1995 , 317-409